Published in final edited form as:
J Am Chem Soc. 2013 September 4; 135(35): 13168–13184. doi:10.1021/ja406608u.

Catalytic Hydrogenation Activity and Electronic Structure Determination of Bis(arylimidazol-2-ylidene)pyridine Cobalt Alkyl and Hydride Complexes

Renyuan Pony Yu[a], **Jonathan M. Darmon**[a], **Carsten Milsmann**[a], **Grant W. Margulieux**[a], **S. Chantal E. Stieber**[a], **Serena DeBeer**[b,c], and **Paul J. Chirik**

Paul J. Chirik: pchirik@princeton.edu

[a]Department of Chemistry, Princeton University, Princeton, New Jersey, U. S. A. 08544

[b]Max-Planck Institute for Chemical Energy Conversion, Stiftstrasse 34-36, D-45470 Mülheim an der Ruhr, Germany

[c]Department of Chemistry and Chemical Biology, Cornell University, Ithaca, New York 14853, United States

Abstract

The bis(arylimidazol-2-ylidene)pyridine cobalt methyl complex, (^{iPr}CNC)CoCH$_3$, was evaluated for the catalytic hydrogenation of alkenes. At 22 °C and 4 atm of H_2 pressure, (^{iPr}CNC)CoCH$_3$ is an effective pre-catalyst for the hydrogenation of sterically hindered, unactivated alkenes such as *trans*-methylstilbene, 1-methyl-1-cyclohexene and 2,3-dimethyl-2-butene, representing one of the most active cobalt hydrogenation catalysts reported to date. Preparation of the cobalt hydride complex, (^{iPr}CNC)CoH was accomplished by hydrogenation of (^{iPr}CNC)CoCH$_3$. Over the course of 3 hours at 22 °C, migration of the metal-hydride to the 4-position of the pyridine ring yielded (4-H$_2$-^{iPr}CNC)CoN$_2$. Similar alkyl migration was observed upon treatment of (^{iPr}CNC)CoH with 1,1-diphenylethylene. This reactivity raised the question as to whether this class of chelate is redoxactive, engaging in radical chemistry with the cobalt center. A combination of structural, spectroscopic and computational studies was conducted and provided definitive evidence for bis(arylimidazol-2-ylidene)pyridine radicals in reduced cobalt chemistry. Spin density calculations established that the radicals were localized on the pyridine ring, accounting for the observed reactivity and suggest a wide family of pyridine-based pincers may also be redox active.

Introduction

The hydrogenation of carbon-carbon multiple bonds catalyzed by homogeneous transition metal complexes is one of the most widely employed reactions in the synthesis of commodity and fine chemicals.[1] There has been renewed interest in developing catalysts using earth abundant elements as alternatives or even improvements to more commonly used precious metal compounds.[2,3] One potential challenge to the discovery of catalysts based on first row metals is the difference in redox properties compared to their second and third row congeners. In catalytic hydrogenation and related processes such as hydrosilylation and hydroboration, important bondbreaking and making processes such as oxidative addition and reductive elimination often rely on two-electron changes.[4] First row

Correspondence to: Paul J. Chirik, pchirik@princeton.edu.

Supporting Information Available. Crystallographic data for (^{iPr}CNC)CoCl, (4-CPh$_2$CH$_3$-^{iPr}CNC)CoN$_2$, [(^{iPr}CNC)CoN$_2$][BAr$^F_4$] and [(^{iPr}CNC)CoCH$_3$] [BAr$^F_4$] in cif format. This material can be downloaded, free of charge, via the internet at http://pubs.acs.org.

metals often engage in one-electron chemistry, offering alternative pathways that disrupt desired transformations required for catalytic turnover.[5]

Two strategies have predominated in overcoming the preference for one-electron redox chemistry associated with base metals to achieve catalysis. The first and most established method is the use of highly covalent, strong field ligands that favor low spin configurations and higher metal oxidation states.[6] The rich and continually evolving catalytic chemistry observed with thermal and photoactivated $Fe(CO)_5$ and $Fe_2(CO)_9$ supports the viability of this approach.[7,8] A second strategy employs redox-active ligands – those that can engage in reversible one-electron chemistry with the transition metal.[9,10,11] By enabling cooperative metal-ligand redox events, net two-electron chemistry can be achieved while the metal engages in only one-electron processes.[12] This concept, important in the function of many metalloenzymes,[13] has emerged as an effective strategy in base metal catalysis,[2a,10,12,14,15] small molecule activation and group transfer chemistry.[16,17]

Aryl-substituted bis(imino)pyridine iron dinitrogen complexes have proven to be effective pre-catalysts for alkene hydrogenation,[18,19] hydrosilylation,[18,20,21] cycloaddition[22,23,24] and hydroboration[25,26] reactions. In many cases, the activity and selectivity of these compounds rivals or surpasses established precious metal catalysts.[27] Notably, introduction of electron donating substituents into the 4-position of the pyridine ring increased the activity for alkene hydrogenation[28] and hydrosilylation.[20b] For example, (4-Me_2N-^{iPr}PDI)$Fe(N_2)_2$[29] exhibited higher turnover frequencies than the first generation pre-catalyst, (^{iPr}PDI)$Fe(N_2)_2$ (^{iPr}PDI = 2,6-(2,6-$^{i}Pr_2$-C_6H_3-N=CMe)$_2C_5H_3N$) in both reaction types (Scheme 1). These findings prompted study of even more electron rich iron bis(dinitrogen) complexes. Danopoulos and coworkers reported the synthesis of (^{iPr}CNC)$Fe(N_2)_2$ (^{iPr}CNC = 2,6-(2,6-$^{i}Pr_2$-C_6H_3-imadazol-2-ylidene)$_2$-C_5H_3N)[30] and infrared stretching frequencies of the N_2 ligands establish a more electron rich iron center than in the corresponding bis(imino)pyridine compounds. Accordingly, (^{iPr}CNC)$Fe(N_2)_2$ and its less sterically protected variants, (^{Me}CNC)$Fe(N_2)_2$ and (^{Mes}CNC)$Fe(N_2)_2$, are extremely active hydrogenation pre-catalysts. The latter compounds exhibit rapid turnover for unactivated tri-and tetrasubstituted alkenes, challenging substrates for even the most active precious metal catalysts.[31]

Cobalt compounds have also demonstrated considerable promise for alkene hydrogenation. Historically, cobalt-catalyzed alkene hydrogenation has been accomplished using borohydrides or hydrogen as the terminal reductant although activities and selectivities are generally low.[32] Budzelaar and coworkers have since reported that four-coordinate, aryl- and alkyl-substituted bis(imino)pyridine cobalt alkyl and hydride complexes, (PDI)CoR,[33,34] are active for the hydrogenation of simple, unactivated terminal and *gem*-alkenes; more sterically hindered trisubstituted olefins are unreactive.[35] Our laboratory has prepared enantiopure, C_1-symmetric variants of these compounds and observed asymmetric hydrogenation of styrenyl-substituted olefins with high enantioselectivity.[36] Hanson and coworkers have recently reported a cobalt(II) alkyl complex supported by a [PNP]-type pincer ligand that is active for the hydrogenation of olefins, ketones, aldehydes and imines[37] as well as for the acceptorless dehydrogenation of alcohols.[38] This catalyst class offers tolerance to a range of functional groups, although hydrogenation of sterically hindered substrates such as tri- and tetrasubstituted olefins remains a challenge.[39]

The similarity between bis(imino)pyridines and the bis(arylimidazol-2-ylidene)pyridines and the improved catalytic performance for alkene hydrogenation observed with iron dinitrogen complexes of the latter pincer class[28] prompted evaluation of the corresponding cobalt alkyl compounds. Danopoulos and coworkers have previously reported the synthesis of (^{iPr}CNC)$CoCH_3$ by treatment of (^{iPr}CNC)CoBr with methyllithium.[40] While this compound was evaluated for ethylene polymerization activity, catalytic alkene hydrogenation studies,

to our knowledge, were not reported. Here we describe the catalytic hydrogenation of sterically hindered alkenes using bis(arylimidazol-2-ylidene)pyridine cobalt complexes. The high activity of the cobalt pre-catalysts raised the question as to the electronic structure of the compounds and if this class of pincer ligand engages in radical chemistry with a reduced base metal. A combined spectroscopic and computational study clearly established the presence of ligand-centered radicals and migration of hydrides and alkyls to the 4-position of the pyridine, supporting this view of the electronic structure.

Results and Discussion

I. Evaluation of Catalytic Performance

Our studies commenced with evaluation of the bis(arylimidazol-2-ylidene)pyridine cobalt methyl complex, (^{iPr}CNC)$CoCH_3$ for the catalytic hydrogenation of a series of alkenes. A summary of the observed hydrogenation activity is reported in Table 1. A comparison to previously reported (^{iPr}CNC)$Fe(N_2)_2$-catalyzed alkene hydrogenation[28] is also presented in the table. Each catalytic hydrogenation was conducted under standard conditions employing 5 mol% of the metal pre-catalyst, 0.916 M substrate in benzene with 4 atm of H_2 at 22 °C. The conversion to alkane was determined by gas chromatography and ^{1}H NMR spectroscopy.

The first substrate examined was ethyl 3,3-dimethylacrylate (entry 1) as this alkene has been used as a benchmark for iron-catalyzed olefin hydrogenation.[19,28] The cobalt methyl pre-catalyst, (^{iPr}CNC)$CoCH_3$, exhibits comparable activity to (^{iPr}CNC)$Fe(N_2)_2$, completing the hydrogenation in one hour under standard conditions. Because of the high activity, only more challenging, unfunctionalized hindered alkenes were examined. The trisubstituted alkenes, *trans*-methylstilbene (entry 2), 2-methyl-2-butene (entry 3), the isomers of β-methylstyrene (entry 5) and 2,6dimethyl-2-octene(entry 6) were also readily hydrogenated. Each substrate reached complete conversion over the course of hours. Hydrogenation of 1-methyl-1-cyclohexene (entry 7), a traditionally more challenging endo cyclic trisubstituted olefin, was also successful. Approximately 32% hydrogenation to alkane was observed after 12 hours and complete conversion was achieved in 120 hours. Unfortunately, only minimal turnover was observed at 22 °C with the tetrasubstituted olefin, 2,3-dimethyl-2-butene (entry 5). Heating the catalytic reaction to 50 °C resulted in 69% conversion to product after 24 hours. These results demonstrate that (^{iPr}CNC)$CoCH_3$ is a more active pre-catalyst than the corresponding iron dinitrogen complex, (^{iPr}CNC)$Fe(N_2)_2$ and is one of the most active base metal alkene hydrogenation catalysts known, proving effective for unactivated, sterically hindered alkenes.[41]

II. Synthesis, Characterization and Reactivity Studies of a Bis(arylimidazol-2-ylidene)pyridine Cobalt Hydride

The high catalytic hydrogenation activity of the (^{iPr}CNC)$CoCH_3$ pre-catalyst prompted study of the corresponding cobalt hydride, a likely component of the catalytic cycle. Exposure of a 25 mM benzene-d_6 solution of (^{iPr}CNC)$CoCH_3$ to 1 atm of hydrogen gas resulted in rapid liberation of CH_4 (as judged by ^{1}H NMR spectroscopy) and formation of a new, diamagnetic C_{2v} symmetric compound identified as the desired cobalt hydride, (^{iPr}CNC)CoH (Scheme 2).

The benzene-d_6 ^{1}H NMR resonances for the chelate in (^{iPr}CNC)CoH are similar to those for (^{iPr}CNC)$CoCH_3$ with the hydrogen in the 4-position of the pyridine located downfield at 11.3 ppm. The Co-H resonance was observed as a very broad ($\nu_{1/2} \sim 148$ Hz) signal whose chemical shift is dependent on the amount of excess dihydrogen present. In a rigorously degassed sample, the peak appears at −27 ppm while in the presence of 1 atmosphere of H_2 this resonance shifts to −18 ppm with additional broadening. A slight broadening of the 4-

pyridine and imidazole positions accompanies the downfield shift, consistent with rapid exchange between the Co-H and free H_2 on the NMR timescale.

Addition of D_2 to a 25 mM benzene-d_6 solution of (^{iPr}CNC)CoCH$_3$ resulted in rapid liberation of an 87:13 ratio of CH_3D and CH_4 along with formation of (^{iPr}CNC)CoD. The observation of CH_4 likely arises from competitive isopropyl aryl group cyclometallation. Continued exposure to excess D_2 resulted in selective incorporation of the isotopic label into the 4-position of the pyridine, one of the imidazolylidene C-H bonds (adjacent to the pyridine) and one of the isopropyl methyl groups (Scheme 2). The rate of deuterium incorporation into the isopropyl methyl and imidazolylidene positions was significantly faster than the pyridine 4-position. Complete deuteration of these positions was accomplished after approximately six hours with periodic agitation of the J. Young NMR tube after which time the Co-H was no longer observed.

Allowing a benzene-d_6 solution of (^{iPr}CNC)CoH to stand at 22 °C under an N_2 atmosphere resulted in conversion to a new C_{2v} symmetric cobalt compound over the course of 3 hours. The toluene solution infrared spectrum exhibited a strong band centered at 2048 cm^{-1} signaling dinitrogen coordination. Notable resonances in the benzene-d_6 ^{1}H NMR spectrum include two triplets centered at 3.57 and 4.31 ppm signaling formation of allylic and vinylic protons due to modification of the pyridine ring. The spectroscopic data in conjunction with structural characterization of related compounds (*vida infra*) establish the identity of the purple-blue product as (4-H$_2$-^{iPr}CNC)CoN$_2$, arising from migration of the cobalt hydride to the *para*-pyridine position of the bis(arylimidazol-2-ylidene)pyridine chelate. The assignment of the allylic resonances was also confirmed by isotopic labeling, whereby (^{iPr}CNC)CoD was synthesized and then converted to (4-H,D-^{iPr}CNC)CoN$_2$. The migration of the cobalt hydride to the 4-position of the pyridine ring is suppressed by excess dihydrogen (or dideuterium). In this matter, isotopic labeling experiments could be conducted to determine the fate of the Co-D during formation of (4-H,D-^{iPr}CNC)CoN$_2$. During the course of these investigations, we also discovered that (4-H$_2$-^{iPr}CNC)CoN$_2$ could also be prepared by treatment of (^{iPr}CNC)CoBr with NaBEt$_3$H.

In solution, (4-H$_2$-^{iPr}CNC)CoN$_2$ proved to be unstable, slowly undergoing decomposition over the course of days even at temperatures as low as −35 °C. This instability has thus far inhibited the isolation of single crystals for X-ray diffraction. Nevertheless, solutions of the compound could be generated by hydrogenation of (^{iPr}CNC)CoCH$_3$ and used for subsequent reactivity studies. It was of interest to determine whether the newly formed C-H bond in the 4-position of the pyridine ring was subject to abstraction. Addition of one equivalent of Ph$_3$CCl to a toluene solution of (4-H$_2$-^{iPr}CNC)CoN$_2$ at −35 °C resulted in an immediate color change from deep blue to brown. Analysis of the product mixture by ^{1}H NMR spectroscopy established formation of (^{iPr}CNC)CoCl and a stoichiometric quantity of Ph$_3$CH (Scheme 2). The cobalt complex was isolated in 74% yield and was also characterized by X-ray diffraction. The overall molecular geometry and metrical parameters are similar to those previously reported for (^{iPr}CNC)CoBr.[40] A representation of the molecular structure is presented in the Supporting Information and selected bond distances are presented in the electronic structure section of the manuscript. Importantly, the reactivity with Ph$_3$CCl demonstrates the ability of the functionalized bis(arylimidazol-2-ylidene)pyridine chelate to participate in cooperative metal-ligand reactivity where removal of a C-H bond is coupled with formation of a cobalt-chloride bond.

The reactivity of (^{iPr}CNC)CoH with alkenes was explored to gain insight into insertion behavior relevant to catalytic hydrogenation. Addition of a slight excess (3.5 equivalents) of 1-butene or isobutene to benzene-d_6 solutions of (^{iPr}CNC)CoH furnished (^{iPr}CNC)CoCH$_2$(CH$_2$)$_2$CH$_3$ and (^{iPr}CNC)CoCH$_2$CH(CH$_3$)$_2$, respectively (eq 1). Both

compounds were characterized by ^{1}H and ^{13}C NMR spectroscopy and established preference for the metal-alkyl derived from 1,2-insertion of the alkene into the cobalt-hydride. Over the course of 48 hours under a dinitrogen atmosphere at 22 °C in benzene-d_6 solution both compounds decompose to an intractable mixture of cobalt products.The rate of decomposition is accelerated if the samples are stored under vacuum. Notably, there was no evidence for migration of the alkyl group to the 4-position of the pyridine ring.

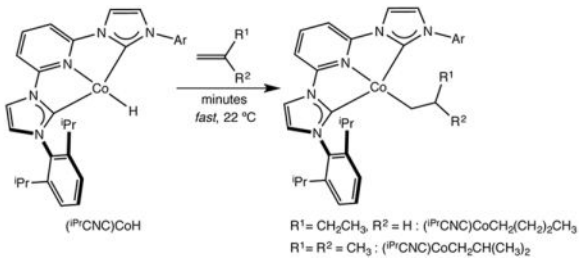

(1)

Insertion studies were also conducted with a more hindered 1,1-disubstituted olefin. Addition of one equivalent of 1,1-diphenylethylene to a 25 mM benzene-d_6 solution of (^{iPr}CNC)CoH under an N_2 atmosphere resulted in a rapid color change from yellow-brown to deep blue. Analysis of a benzene-d_6 solution of the product by IR spectroscopy revealed a strong band centered at 2050 cm^{-1}, again signaling dinitrogen coordination. The benzene-d_6 ^{1}H NMR spectrum exhibited the number of resonances consistent with C_s symmetry. As with (4-H_2-^{iPr}CNC)CoN_2, a doublet and triplet were observed at 4.33 and 4.90 ppm, respectively, signaling modification of the pyridine ring. The combined IR and NMR data support formation of (4-CPh_2CH_3-^{iPr}CNC)CoN_2, arising from migration of the alkyl to the 4-position of the pyridine ring (eq 2).

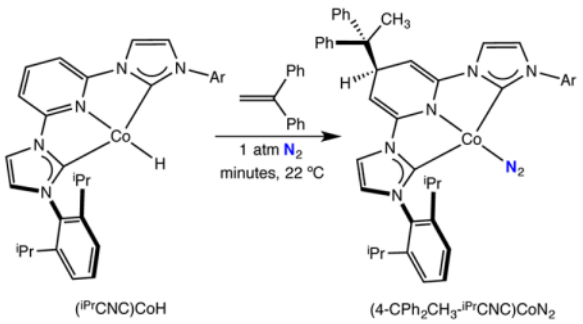

(2)

The modification of the pyridine ring in (4-CPh_2CH_3-^{iPr}CNC)CoN_2 was confirmed by X-ray diffraction. A representation of the molecular structure is presented in Figure 1 and selected bond distances and angles are reported in Table 2. The overall molecular geometry about the metal is best described as idealized planar, as anticipated for a formally Co(I), d^8 center. The aryl substituents are nearly orthogonal to the idealized metal-chelate plane and the N(6)-N(7) distance of 1.112(2) Å signals weak activation of the N_2 ligand. The 4-position of the central pyridine ring is substituted with an alkyl ligand resulting from a new bond between C(6) and C(36), the more substituted carbon of the alkene forming a

quaternary center. The C(5)-C(6) and C(6)-C(7) distances are elongated to 1.513(3) and 1.526(2) Å consistent with formation of an sp^3 hybridized carbon in the 4-position although C(6) deviates little from the idealized plane of the heterocycle.

One possibility accounting for the formation of (4-CPh_2CH_3-^{iPr}CNC)CoN_2 is 2,1-insertion of the alkene into the cobalt-hydrogen bond followed by migration of the alkyl to the 4-position of the pyridine ring. Migration of alkyl groups to the 4-position of related bis(imino)pyridines has been observed by Cámpora and coworkers in manganese chemistry and has been evolved into a useful synthetic method for the preparation of 4-alkyl substituted variants of these ligands.[42] The preference for 2,1 insertion of 1,1-diphenylethylene contrasts the 1,2-insertion preference observed with 1-butene and isobutene. In rhodium chemistry, Jones and coworkers have rationalized the thermodynamic preference between linear and branched metal alkyls as arising from the relative strengths of the newly formed β-C-H bonds.[43] It is likely that for the cobalt complexes described here, the preference for formation of a methyl C-H bond over a methine C-H is larger for 1,1-diphenylethylene than for 1-butene (methylene) or isobutene. The resulting tertiary cobalt alkyl is sufficiently sterically pressured to undergo homolysis and the resultant stabilized radical then adds to the 4-position of the pyridine ring. Notably, 1,1-diphenylethylene undergoes catalytic hydrogenation[44] and was completely converted to the corresponding alkane in the presence of 5 mol% (^{iPr}CNC)$CoCH_3$ and 1 atm of H_2 over the course of 24 hours.

An alternative pathway to account for formation of (4-CPh_2CH_3-^{iPr}CNC)CoN_2 involves H-atom transfer (HAT) from the cobalt-hydride.[45] Halpern proposed sequential HAT events from in situ generated $(CO)_4CoH$ during the reduction of anthracene[46] and in the hydrogenation of α-methylstyrene with $(CO)_5MnH$.[47] HAT pathways have also been proposed in alkene reductions with chromium,[48,49] tungsten,[50] and vanadium[51] hydrides. Our current data do not allow for distinction of these pathways. However, the observation of the cobalt-hydride and alkyl migration to the 4-position of the pyridine raised the possibility of radical character in bis(arylimidazol-2-ylidene)pyridine chelates and prompted further study of the electronic structure of (^{iPr}CNC)CoX (X = H, alkyl, halide) complexes.

III. Electronic Structure of Bis(arylimidazol-2-ylidene)pyridines Cobalt Complexes

The superior catalytic activity of (^{iPr}CNC)$CoCH_3$ as compared to (^{iPr}CNC)$Fe(N_2)_2$ and related bis(imino)pyridine compounds raised the question as to the electronic structure of the pre-catalyst and the role of the bis(arylimidazol-2-ylidene)pyridine ligand. The observation of hydride and alkyl migration to the 4-position of the chelate also suggested the possibility of radical character in this ligand class. It is now well-established that diamagnetic (^{iPr}PDI^{1-})$Co^{II}CH_3$ is a low spin Co(II) compound engaged in antiferromagnetic coupling with a bis(imino)pyridine radical anion.[52] The similar geometries between (^{iPr}PDI^{1-})$Co^{II}CH_3$ and (^{iPr}CNC)$CoCH_3$ suggest the possibility of similar electronics. Determining the oxidation state of both the metal and the pincer ligand is essential for understanding the mechanism of turnover and raises the broader question as to whether bis(arylimidazol-2-ylidene)pyridine chelates can engage in radical chemistry with an appropriately reducing base metal. To address these issues, a series of spectroscopic, computational and preparative studies were carried out.

A. Evaluation of the Free Ligand

To determine if bis(arylimidazol-2-ylidene)pyridine chelates are redox-active, studies with the free ligand were initially conducted. Our laboratory has recently reported that cyclic voltammetry is one of the most sensitive evaluators of the electronic properties of aryl-substituted bis(imino)pyridines.[53,54,55] Reduction potentials between −2.35 and −2.83 V (vs

Fc/Fc^{+}) were observed in THF solution depending on the specific substitution pattern of the bis(imino)pyridine. Performing identical measurements on the free bis(arylimidazol-2-ylidene)pyridine, ^{iPr}CNC,[56] in THF solution (1 mM ^{iPr}CNC in 0.1 M $[^{n}Bu_4]PF_6$ electrolyte) were unsuccessful as no reversible redox waves were observed, suggesting a less thermodynamically accessible radical anion for this ligand class.

Despite the lack of success with electrochemical reduction, access to the desired bis(arylimidazol-2-ylidene)pyridine radical anion was explored chemically. For spectroscopic reference, alkali metal salts of previously reported aryl-substituted bis(imino)pyridine radical anions[57] were initially synthesized to evaluate various synthetic routes as well as to compare EPR spectroscopic signatures. Stirring THF solutions of the free chelates with excess sodium resulted in formation of red-purple solutions identified as Na[(^{iPr}PDI] and Na[(^{iPr}BPDI)], respectively (^{iPr}BPDI= 2,6-(2,6-$^{i}Pr_2$-C_6H_3N=CPh)$_2C_5H_3N$). After dilution with toluene (toluene/THF ~ 10:1) the samples were investigated by X-band EPR spectroscopy at 298 K (Figure 2). The spectrum obtained for Na[(^{iPr}BPDI)] exhibits a sharp isotropic signal centered at g_{iso} = 2.003 with ten resolved lines due to hyperfine coupling. Examples of EPR spectra of bis(imino)pyridine radicals coordinated to diamagnetic metal ions have been reported previously by Gambarotta and coworkers for (^{iPr}PDI)$AlMe_2$,[58] our laboratory for (^{iPr}BPDI)VE_2 (E = O, S, NPh)[59] and (^{iPr}PDI)CoN_2.[60] These studies established that the major contributions to the hyperfine coupling pattern arise from the nitrogen and hydrogen nuclei constituting the plane of the bis(imino)pyridine ligand with additional contributions from the metal center as expected for a radical delocalized over the conjugated π-system of the chelate. Given these precedents, the EPR spectrum of Na[(^{iPr}BPDI)] was readily simulated assuming hyperfine coupling to the pyridine and imine nitrogen nuclei ($A_{iso}(^{14}N_{py})$ = 6.2 MHz, $A_{iso}(^{14}N_{im})$ = 3.3 MHz), the *para*-pyridine proton ($A_{iso}(^{1}H_{para})$ = 14.0 MHz), and the sodium cation ($A_{iso}(^{23}Na)$ = 8.4 MHz). In agreement with the previous studies and related efforts with pyridine radical anions,[61] the largest contributions to the hyperfine coupling arises from coupling to the proton in the 4-position of the pyridine ring, while contributions from the protons in the 3-position are small and not resolved in the recorded spectrum of Na[(^{iPr}BPDI)]. It should be noted that the observed ten line pattern is merely the envelope of a more complex hyperfine pattern that is not further resolved due to line broadening. Assuming only contributions from the H, N, and Na nuclei of the chelate plane, a total of 360 resonances is expected for a complex with C_s symmetry or higher. This number increases for the EPR spectrum of Na[(^{iPr}PDI)] due to contributions from the in plane methyl substituents of the chelate backbone producing a theoretical maximum of 2520 lines. Indeed, the recorded isotropic spectrum centered at g_{iso} = 2.003 for Na[(^{iPr}PDI)] exhibits a pattern that is similar to the spectrum of Na[(^{iPr}BPDI)] split by additional hyperfine features. Unfortunately, we have not been able to obtain a satisfactory fit of the data due to the high complexity of the hyperfine pattern.

Similar studies were conducted with the bis(arylimidazol-2-ylidene)pyridine, ^{iPr}CNC. Stirring the free dicarbene with excess sodium metal in THF immediately produced an orange solution. Analysis by EPR spectroscopy established the formation of a paramagnetic product assigned as Na[^{iPr}CNC] (Figure 3). An alternative route, whereby $CNC(HBr)_2$[62] was treated with excess sodium, proved less reliable and generated unidentified byproducts. Similar to the bis(imino)pyridine radicals, the X-band EPR spectrum of Na[^{iPr}CNC] centered at g_{iso} = 2.003 exhibits the complexity expected for an organic radical delocalized over the π-system of the pyridine and NHC rings. Again assuming hyperfine contributions from the in-plane N, H, and Na nuclei of the complex, a maximum number of 16200 resonances are possible, giving rise to the observed multi-line pattern. Computational studies (see below) reveal that the spin density in the [^{iPr}CNC] radical anion are mostly localized on the pyridine ring suggesting that hyperfine contributions from the imidazole nuclei are small

compared to contributions from the pyridine ring and the metal cation. However, the multitude of small contributions adds to the line broadening of the spectrum, thus lowering the resolution and complicating simulations of the data.

In an attempt to simplify the hyperfine structure of the [^{iPr}CNC] radical anion, alternative reductants were explored to replace the sodium cation (100% ^{23}Na, $I = 3/2$) by a nonmagnetic cation. Stirring a THF slurry of $CNC(HBr)_2$ with excess magnesium powder in the presence of catalytic amounts of anthracene[63] generated an orange solution identified as MgBr[(^{iPr}CNC)] (Figure 3, top). The X-band EPR spectrum exhibits an isotropic signal (g_{iso} = 2.003) consistent with an $S = 1/2$ organic radical. As expected, the introduction of the predominantly nonmagnetic magnesium nucleus (90% $^{24/26}$Mg, $I = 0$; 10% ^{25}Mg, $I = 5/2$) simplifies the data significantly producing a spectrum with a 14-line main feature and additional small signals visible at the edges of the spectrum arising from coupling to ^{25}Mg. Despite the smaller number of potential hyperfine lines (4050) the spectrum of MgBr[(^{iPr}CNC)] covers a slightly wider field range, which is most likely due to small changes in the spin distribution over the π-system induced by Mg as compared to Na resulting in slightly different coupling constants for the N and H nuclei. Unfortunately, a satisfactory simulation could not be obtained even for the simplified spectrum of the magnesium derivative.

B. Synthesis of Additional Bis(arylimidazol-2-ylidene)pyridine Cobalt Complexes

Additional bis(arylimidazol-2-ylidene)pyridine cobalt compounds were synthesized as references for structural and spectroscopic measurements. Previous studies with bis(imino)pyridine cobalt complexes served as a guide for specific cobalt derivatives. Gibson[34] and our laboratory[60,64] have established that the cationic bis(imino)pyridine cobalt dinitrogen complex, [(^{iPr}PDI)CoN_2]$^+$ is a low-spin Co(I), d^8 compound with a neutral, redox-innocent chelate. Likewise, one electron oxidation of (^{iPr}PDI^{1-})Co$^{II}CH_3$ is ligand-based, furnishing [(^{iPr}PDI^0)Co$^{II}CH_3$]$^+$, an overall $S = 1/2$ compound best described as low-spin Co(II) with a neutral bis(imino)pyridine.[65] EPR studies on the latter support this view with identification of a cobalt-centered spin. Inspired by these findings, the synthesis of the analogous bis(arylimidazol-2-ylidene)pyridine cobalt cations was explored.

Addition of $NaBAr^F_4$ to a diethyl ether solution of (^{iPr}CNC)CoBr under a dinitrogen atmosphere followed by recrystallization from pentane-fluorobenzene yielded a bright green diamagnetic solid identified as [(^{iPr}CNC)CoN_2][BAr^F_4] (BAr^F_4 = B(3,5-$(CF_3)_2C_6H_3)_4$) in 92% yield (eq 3). The toluene solution infrared spectrum of [(^{iPr}CNC)CoN_2][BAr^F_4] exhibits a strong band at 2141 cm^{-1}, signaling dinitrogen coordination. The ^{1}H and ^{13}C NMR spectra recorded in fluorobenzene-d_5 are consistent with a C_{2v} symmetric molecule. The compound was characterized by single crystal X-ray diffraction and a representation of the molecular structure is presented in Figure 4. Selected metrical parameters for this and all of the bis(arylimidazol-2-ylidene)pyridine cobalt compounds crystallographically characterized for electronic structure elucidation are presented in Table 3. The crystallographic data establishes a planar cobalt dinitrogen complex with no close contacts between the cation and anion (see Supporting Information).

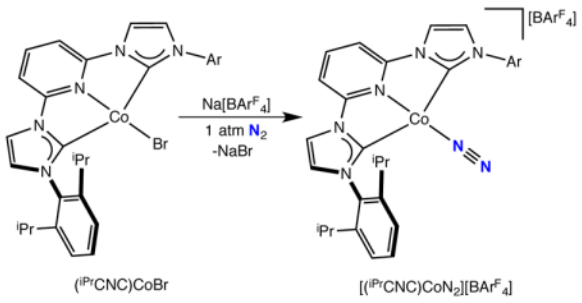

(3)

A second example of a compound expected to have a neutral, redox innocent bis(arylimidazol-2-ylidene)pyridine was [(^{iPr}CNC)CoCH$_3$][BAr$^F_4$]. Oxidation of (^{iPr}CNC)CoCH$_3$ with [Cp$_2$Fe][BAr$^F_4$] in fluorobenzene furnished blue-green crystals identified as the desired cobalt methyl cation, [(^{iPr}CNC)CoCH$_3$][BAr$^F_4$] in 15% isolated yield (eq 4).

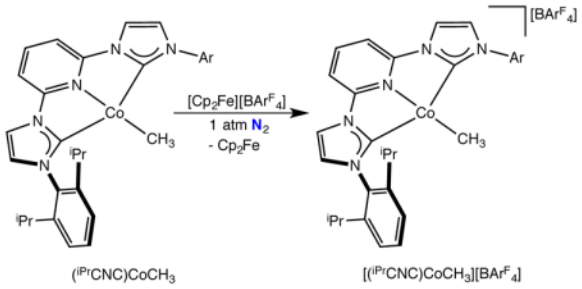

(4)

A solution (Evans method) magnetic moment of 1.8(5) μB was measured at 22 °C, establishing an S = 1/2 ground state. Accordingly, the EPR spectrum (Figure 5) recorded on a solid powder sample at 10 K exhibits a rhombic signal, consistent with the observed doublet state. The spectrum was successfully simulated assuming g values of g_x = 3.36, g_y = 2.43, g_z = 1.85 and hyperfine coupling to ^{59}Co (100%, I = 7/2, A_{xx} = 1062 MHz, A_{yy} = 581 MHz, A_{zz} = 494 MHz). The remarkable anisotropy of the g tensor and the large hyperfine coupling constants demonstrate a cobalt-centered spin consistent with previous reports on the EPR spectra of square-planar Co(II) complexes.[66]

The solid-state structure was determined by X-ray diffraction and a representation of the molecule is presented in Figure 6. The crystallographic data confirm the identity of the compound as [(^{iPr}CNC)CoCH$_3$][BAr$^F_4$] and there are no close contacts between the cation and anion (see Supporting Information). The sum of the angles about the metal center is 359.96(8)°, indicating a idealized planar compound.

Examples of compounds with the potential of adopting one-electron reduced chelates were of particular interest to determine whether bis(arylimidazol-2-ylidene)pyridines are redox active. Previous studies with bis(imino)pyridine compounds identified (^{iPr}PDI)CoN$_2$ as a low-spin Co(I), d^8 compound with a one-electron reduced chelate accounting for the observed S = 1/2 ground state.[60] The toluene solution EPR spectrum of the compound

recorded at 298 K experimentally verified the ligand-centered radical as the SOMO of the molecule thereby providing definitive evidence for the redox-activity of this ligand class. Accordingly, the bis(arylimidazol-2-ylidene)pyridine analog, (^{iPr}CNC)CoN$_2$ was targeted for synthesis and electronic structure determination.

Attempts to prepare the desired neutral cobalt dinitrogen compound by reduction of (^{iPr}CNC)CoBr with sodium amalgam yielded a mixture of cobalt products with (4-H$_2$-^{iPr}CNC)CoN$_2$ as the only identifiable compound. Performing the reduction with sodium metal in the presence of 5 mol% of naphthalene also furnished a mixture of products from which (4-H$_2$-^{iPr}CNC)CoN$_2$ and Na[^{iPr}CNC] were identified. By contrast, stirring a toluene or benzene solution of [(^{iPr}CNC)CoN$_2$][BAr$^F_4$] in the presence of one equivalent of (η^5-C$_5$Me$_5$)$_2$Co for 10 minutes yielded a blue-green solution. Monitoring the reaction by infrared spectroscopy established that all of the [(^{iPr}CNC)CoN$_2$][BAr$^F_4$] is consumed with concomitant appearance of a band centered at 2047 cm^{-1}, signaling formation of the neutral cobalt dinitrogen complex, (^{iPr}CNC)CoN$_2$ (eq 5).

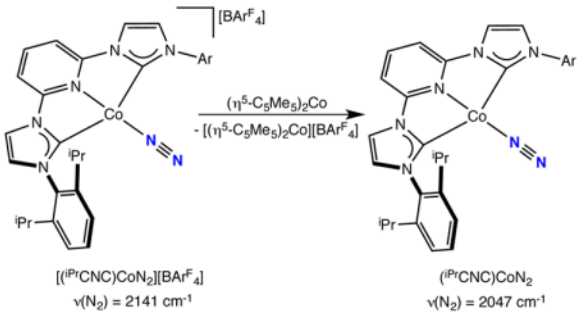

(5)

Analysis of the in situ generated product by EPR spectroscopy in benzene solution at 298 K established an S = 1/2 compound, similar to (^{iPr}PDI)CoN$_2$. The observed isotropic signal at g_{iso} = 1.998 exhibits eight partially overlapped hyperfine lines, arising from coupling of the principally ligand-centered radical to the I = 7/2 ^{59}Co nucleus (Figure 7). Simulation of the data established an isotropic hyperfine coupling constant, A_{iso} = 36 MHz. No hyperfine coupling to hydrogen or nitrogen atoms was observed, which can be attributed to increased line broadening due to coordination of the ligand radical to the cobalt center, as observed for the ^{iPr}PDI analog.[60] The A_{iso} is similar to that observed in previously reported (^{iPr}PDI)CoN$_2$ (24 MHz), supporting an electronic structure description of a low-spin Co(I) ion with a [^{iPr}CNC]$^{1-}$ chelate radical anion. Unfortunately, (^{iPr}CNC)CoN$_2$ underwent rapid decomposition in solution to an unidentified S = 1/2 cobalt compound. The spectrum was simulated with the presence of an S = 1/2 species centered at g_{iso} = 2.00 at 40% ratio. A time course of the decomposition as measured by EPR spectroscopy is reported in the Supporting Information.

C. Analysis of the Metrical Parameters of Structurally Characterized Bis(arylimidazol-2-ylidene)pyridine Cobalt Complexes

Distortions to the metrical parameters of a chelating ligand has been established as a diagnostic tool for establishing redox activity.[67,68] Supporting these observations with computational and spectroscopic studies is useful for determining the spectroscopic oxidation state of redox-active transition metal compounds. Because several bis(arylimidazol-2-ylidene)pyridine cobalt complexes have now been structurally

characterized, meaningful analysis can be carried out to establish the bond distances associated with the neutral and one electron reduced forms of the ligand. As will be presented in a subsequent section of the manuscript, the established ranges have also been computationally verified.

Selected bond distances for structurally characterized bis(arylimidazol-2-ylidene)pyridine cobalt complexes are presented in Table 3. Also presented in Table 3 are the metrical parameters of the free chelate as a reference and comparison. Computational studies (*vide infra*) and resonance structures allow prediction of the distortions to the chelate. Illustrated in the table is the DFT computed b_2 molecular orbital of the bis(arylimidazol-2-ylidene)pyridine radical anion that highlights the expected bond elogations and contractions. Reduction of the bis(arylimidazol-2-ylidene)pyridine pincer results in elongations and contractions to the central pyridine ring as well as an elongation of $C_{carbene}$-N_{imid} distances. Within the pyridine ring, the N_{pyr}-C_{ipso} and C_{meta}-C_{para} distances are expected to elongate upon addition of an electron while C_{ipso} -C_{meta} bonds contract.

In the free bis(arylimidazol-2-ylidene)pyridine (^{iPr}CNC), [(^{iPr}CNC)CoCH$_3$][BAr$^F_4$], and [(^{iPr}CNC)CoN$_2$][BAr$^F_4$], the N_{pyr}-C_{ipso} distances range between 1.327(4) and 1.345(5) Å. In the cobalt monohalide and methyl complexes, this length range expands to 1.353(7) to 1.371(7) Å, consistent with one electron reduction of the chelate. The C_{meta}-C_{para} distances also exhibit distortions, albeit slightly less pronounced, ranging between 1.384(5)-1.392(5) Å in the redox innocent compounds that elongate to 1.392(5)-1.416(6) Å in the (^{iPr}CNC^{1-})Co^{II}X derivatives. The anticipated contraction of the C_{ipso}-C_{meta} distances is apparent but less definitive. In the redox innocent compounds, values range between 1.362(5)-1.388(5) Å and are altered to 1.367(4)-1.378(8) Å in the (^{iPr}CNC^{1-})Co^{II}X examples. It should be noted that the lower limit of the redox innocent range is skewed by one anomalous value in the structure of the free bis(arylimidazol-2-ylidene)pyridine. If this value is discarded, the range for the neutral ligand becomes 1.375(4)-1.388(5) Å. The $C_{carbene}$-N_{aryl} distances also exhibit distortions, ranging between 1.346(2)-1.359(4) Å in redox innocent compounds and elongate to 1.360(7)-1.386(6) Å in the reduced chelate. The distortions in bond distances was also anticipated from examination of the calculated b_2 orbital of [CNC]$^{1-}$ chelate, which clearly establishes anti-bonding character at elongated positions. Taken together, the crystallographic data clearly establish that the (^{iPr}CNC^{1-})Co^{II}X family of compounds, much like their bis(imino)pyridine counterparts, contain radical bis(arylimidazol-2-ylidene)pyridine chelates and low-spin cobalt(II) centers.

D. X-ray Absorption Studies

The single crystal X-ray diffraction data for both (^{iPr}CNC)CoBr and (^{iPr}CNC)CoCH$_3$ are consistent with low-spin Co(II) complexes with bis(arylimidazol-2- ylidene)pyridine radical anions. To further support this view of the electronic structure, X-ray absorption spectroscopic (XAS) studies were conducted (Figure 8). This study also included (^{iPr}PDI^{1-})Co^{II}Br and (^{iPr}PDI^{1-})Co^{II}CH$_3$, established low-spin Co(II) compounds with chelate radical anions. The rising edge and pre-edge region of all four compounds fall in a similar energy range (Table 4), supporting the same cobalt oxidation state for all members of the series. For (^{iPr}CNC)CoBr and (^{iPr}PDI)CoCl, the first pre-edge features appear at 7709.8 and 7709.3 eV, respectively, values consistent with those previously reported for Co(II) compounds.[69] The 0.5 eV shift for the bis(arylimidazol-2-ylidene)pyridine derivative is likely due to the greater π-acidity of this chelate relative to the bis(imino)pyridine. The replacement of Cl by Br in the first coordination sphere, however, may also contribute to a decrease in edge energy. Likewise, the pre-edges for (^{iPr}CNC)CoCH$_3$ and (^{iPr}PDI)CoCH$_3$ were observed at 7709.7 eV, and at 7709.3 eV, respectively. Both of the bis(arylimidazol-2-ylidene)pyridine cobalt compounds exhibit an additional pre-edge feature at slightly higher

energy, likely due to a 1*s* to ligand π* transition.[70,71] Collectively, the XAS results support low-spin cobalt(II) compounds with bis(arylimidazol-2-ylidene)pyridine radical anions.

E. ^{1}H NMR Spectroscopic Studies

The NMR spectra of diamagnetic transition metal complexes bearing redox-active ligands has proven valuable in determination of their electronic structure. Budzelaar and coworkers[52,74] and subsequently our laboratory[60,70,75] have demonstrated the utility of ^{1}H NMR chemical shifts of the in-plane hydrogens of bis(imino)pyridine chelates to be diagnostic of radical chemistry and participation in the overall electronic structure. Deviations of the in-plane chelate hydrogens from their diamagnetic reference values have been attributed to either thermal population of a triplet excited state[52] or from temperature independent paramagnetism.[75]

Because of the simplicity and insightfulness of the technique, the ^{1}H NMR spectrum of (^{iPr}CNC)CoCH$_3$ was examined in detail. As reported by Danopoulos,[40] the benzene-d_6 ^{1}H NMR spectrum of (^{iPr}CNC)CoCH$_3$ at 22 °C exhibits a downfield shifted resonance at 10.65 ppm for the *para*-pyridine proton. This shift is similar to the value of 10.19 ppm reported for (^{iPr}PDI)CoCH$_3$.[76] The spectra of the two compounds are presented in Figure 9.

The similarity in the ^{1}H NMR shifts of (^{iPr}CNC)CoCH$_3$ and (^{iPr}PDI)CoCH$_3$ are consistent with the other spectroscopic and metrical data that indicate the former is a low spin cobalt(II) compound with a bis(arylimidazol-2-ylidene)pyridine radical anion. Because thermal population of a triplet excited state has been invoked to explain the anomalous chemical shifts of (^{iPr}PDI)CoCH$_3$,[52] variable temperature ^{1}H NMR experiments were performed on a series of (^{iPr}CNC)CoX (Br, CH$_3$, H) compounds in toluene-d_8. Stack plots of the spectra are reported in the Supporting Information. For both (^{iPr}CNC)CoBr and(^{iPr}CNC)CoCH$_3$, the chemical shifts are invariant with temperature, changing < 0.1 ppm from -70 to 22 °C. Thus, no change in population of the triplet state was detectable by ^{1}H NMR spectroscopy. The hydride compound, (^{iPr}CNC)CoH is anomalous. Almost all of the resonances are invariant with temperature with the exception of the *para*-pyridine, which broadens significantly from −40 °C to 22 °C. This broadening is accompanied by an upfield shift of approximately 0.5 ppm upon warming. Recall, this compound undergoes migration of the metal-hydride to the 4-position of the pyridine and exchange with free H$_2$ and thus we are unable to distinguish the changes in the NMR spectrum resulting from a chemical process or an unusual electronic structure.

The observation of temperature independent chemical shifts in the bis(arylimidazol-2-ylidene)pyridine cobalt bromide and methyl compounds raised the question of similar behavior in (^{iPr}PDI)CoCH$_3$. To our knowledge, the variable temperature NMR data for this compound has not been reported. Over the temperature range of −70 to 40 °C, no significant change in chemical shifts was observed (see Supporting Information for stack plots). Budzelaar and coworkers previously calculated a difference of 7.2 kcal for the energy between the singlet and triplet states for (^{iPr}PDI)CoCH$_3$.[52] Assuming a Boltzman distribution between the states, the abundance of the triplet state at 22 °C is 4.7 × 10^{-4}%. Cooling the sample to −70 °C, decreases this value to 1.8 × 10^{-6}% while warming to 40 °C increases the population 9.4 × 10^{-4}%. That is to say the triplet state of (^{iPr}PDI)CoCH$_3$ is 260 times more abundant at 22 °C than −70 °C and 526 times more abundant at 40 °C than −70 °C.

If thermal population of a triplet excited state is indeed the origin of the anomalous ^{1}H NMR shifts observed at 22 °C, a 4.7 × 10^{-4}% population of the triplet excited state is responsible for shifting the imine methyl groups approximately 3-4 ppm from their diamagnetic reference values. Cooling the sample should decrease this population significantly and

likewise induce a significant shift of the imine methyl group and other in plane hydrogens toward their diamagnetic reference values. Similarly, heating the sample should result in a greater dispersion of these chemical shifts. Because no change was observed over a 110 °C temperature range, we conclude that thermal population of a triplet excited state is not the origin of the anomalous shifts. The more likely explanation is temperature independent paramagnetism, whereby a triplet excited state mixes into the singlet ground state by spin orbit coupling as the resulting ^{1}H NMR chemical shifts are invariant with temperature. Such behavior has been observed in isoelectronic, neutral ligand complexes of bis(imino)pyridine iron.[75,77]

F. Computational Studies

Broken-symmetry[78] DFT computational studies were conducted to corroborate the experimental results and firmly establish the electronic structures of various bis(arylimidazol-2-ylidene)pyridine cobalt compounds. Full molecule calculations and geometry optimizations were conducted in each case at the B3LYP level of DFT. Broken symmetry calculations were performed to describe the open shell singlet configuration of the redox-active cobalt compounds. In the broken symmetry notation BS(m, n) describes a state in which there are m unpaired spin-up electrons and n unpaired spin-down electrons on separate fragments.[78,79,80]

The first class of compounds examined were those expected to have neutral bis(arylimidazol-2-ylidene)pyridine chelates. The two cationic cobalt complexes, $[(^{iPr}CNC)CoN_2]^+$ and $[(^{iPr}CNC)CoCH_3]^+$ were initially explored and only the cationic portion of the molecule was calculated with $S = 0$ and $S = 1/2$ ground states, respectively. The crystallographic data suggest no participation of the chelate in the electronic structure of the compounds. A comparison between the experimental and computational bond distances for both compounds is reported in the Supporting Information.

Calculations on $[(^{iPr}CNC)CoN_2]^+$ were performed using both BS(1,1) and Restricted Kohn-Sham (RKS) formalisms. The BS(1,1) input converged to the close-shell solution identical to the results from the RKS input. A truncated, qualitative molecular orbital diagram is presented in Figure 10 and clearly establishes a low-spin Co(I) complex with a neutral, redox-innocent bis(arylimidazol-2-ylidene)pyridine, consistent with the experimental data. The highest occupied molecular orbital is exclusively cobalt d_{z2}, as expected for a square planar, d^8 metal complex. To provide additional support for the accuracy of the DFT result, a vibrational frequency calculation of the N_2 stretch was performed. This calculation was carried out with the BP86 functional for computational expediency. This calculation predicts the N_2 stretching frequency at 2173 cm^{-1}, in reasonable agreement with the experimental value of 2141 cm^{-1}. Thus both the experimental and computational data support $[(^{iPr}CNC^0)Co^IN_2]^+$ as the best description of the electronic structure.

Computations were also performed on $[(^{iPr}CNC)CoCH_3]^+$ using a doublet ground state as established experimentally. Applying a spin-unrestricted formalism, the calculations converged to an open-shell solution and a comparison of computed and experimental bond distances are reported in the Supporting Information. Presented in Figure 11 is a truncated qualitative molecular orbital diagram along with a Mulliken spin density plot. The computational results clearly support a low-spin Co(II) complex with a redox neutral bis(arylimidazol-2-ylidene)pyridine. The ligand oxidation state is similar to that observed with $[(^{iPr}CNC)CoN_2]^+$. For $[(^{iPr}CNC)CoCH_3]^+$, the SOMO of the molecule is a cobalt d_{z2} molecular orbital, consistent with the observed EPR spectrum for the compound.

Having corroborated the electronic structures of compounds with neutral bis(arylimidazol-2-ylidene)pyridines, cobalt complexes with one electron reduced chelates (*i.e.* $(^{iPr}CNC)CoX$)

were studied. Geometry optimizations were performed with RKS and BS(1,1) inputs at the B3LYP level of DFT. The BS(1,1) solution was found to be 7 kcal/mol lower in energy than the RKS alternative, supporting a redox-active description. The metrical parameters from both calculations are in excellent agreement with the experimentally determined values and are summarized in the Supporting Information.

Examination of the computed molecular orbitals from the open shell singlet solution (Figure 12) revealed a low spin Co(II) complex with three doubly occupied metal *d* orbitals and a SOMO of primarily d_{xz} parentage. The SOMO is engaged in an antiferromagnetic coupling interaction ($S = 0.58$) with an ^{iPr}CNC b_2 molecular orbital. Examination of the Mulliken spin population analysis also corroborates this view of the electronic structure.

Similar studies were also conducted on the cobalt methyl complex, (^{iPr}CNC)$CoCH_3$. As with (^{iPr}CNC)CoBr, a BS(1,1) solution was preferred corresponding to a low-spin cobalt(II) complex and a bis(arylimidazol-2-ylidene)pyridine radical anion. A truncated, qualitative molecular orbital diagram and Mulliken spin population analysis are presented in Figure 13. Three doubly occupied metal *d* orbitals and a SOMO of primarily d_{xz} character are observed. The SOMO is engaged in an antiferromagnetic coupling interaction ($S = 0.48$) with an ^{iPr}CNC b_2 molecular orbital. As with the bromide, the ligand-centered radical is largely pyridine localized.

Presented in Figure 14 is a comparison of the Mulliken spin density of bis(imino)pyridine versus bis(arylimidazol-2-ylidene)pyridine cobalt methyl complexes. It is notable that the radical character on the bis(arylimidazol-2-ylidene)pyridine chelate is largely localized in the pyridine ring with little contribution from the *N*-heterocyclic carbenes. This feature likely accounts for the observed reactivity where metal-hydrides and stabilized alkyl radicals migrate to the 4-position of the ring. In bis(imino)pyridine compounds, significant delocalization over the entire π-system of the chelate is observed and hence analogous migration processes have not been observed in reduced cobalt chemistry (Figure 14).

One final set of time dependent DFT calculations were conducted, using methods previously described,[81] to further understand the observed XAS spectra. Using 50 roots (Figure 15), both closed-shell (RKS) and BS(1,1) inputs were evaluated for (^{iPr}CNC)$CoCH_3$ to determine whether or not XAS could distinguish redox innocent and redox active possibilities. The closed shell solution resulted in no calculated pre-edge transition while the BS(1,1) solution reproduced one pre-edge transition dominated by a transition to the cobalt d_{xz} orbital. These further corroborate the BS(1,1) electronic structure description for (^{iPr}CNC)$CoCH_3$ and firmly establish bis(arylimidazol-2-ylidene)pyridine as a redox-active ligand.

IV. Evaluation of the Catalytic Alkene Hydrogenation Activity of Other Bis(arylimidazol-2-ylidene)pyridine Cobalt Precursors

Determination of the electronic structure of various bis(arylimidazol-2-ylidene)pyridine cobalt compounds prompted evaluation of their catalytic alkene hydrogenation activity. Such studies may ultimately allow for a correlation between redox activity of the supporting ligand and catalytic performance. The hydrogenation of *trans*-methylstilbene was used as a representative catalytic reaction. Each trial was conducted with 5 mol% of the metal complex in a 0.916 M solution of the substrate in the desired solvent under 4 atm of H_2 at 22 °C for one hour. The results of these studies are reported in Table 5.

Because of the poor solubility of [(^{iPr}CNC)CoN_2][BAr^F_4] in hydrocarbon solvents such as benzene, the catalytic performance of the compound was initially evaluated in fluorobenzene. Only 6% conversion to alkane was observed under these conditions. For

comparison, the catalytic activity of (^{iPr}CNC)$CoCH_3$ was also evaluated in fluorobenzene and the conversion was reduced to 14% as compared to 50% in benzene. Accordingly, a method was developed to generate [(^{iPr}CNC)CoN_2][BAr^F_4] in situ in hydrocarbon solvents. A benzene solution of (^{iPr}CNC)CoBr was stirred with a slight excess of $NaBAr^F_4$ and the catalytic hydrogenation of *trans*-methyl stilbene was conducted under standard conditions. Using this method, an improved conversion of 27% was observed after one hour but the observed activity remains inferior to the neutral cobalt methyl compound, (^{iPr}CNC)$CoCH_3$. One final example, the neutral cobalt(I) dinitrogen compound, (4-H_2-^{iPr}CNC)CoN_2 was studied. Only 27% conversion to alkane was observed after one hour under standard conditions, again inferior to the neutral cobalt methyl compound. While it is tempting to correlate electronic structure with catalytic performance, more detailed studies are required to make such assertions as the kinetics of the reaction, number of active sites and stability of the active species may be the origin of the observed differences.

Concluding Remarks

The bis(arylimidazol-2-ylidene)pyridine cobalt methyl complex, (^{iPr}CNC)$CoCH_3$, was found to be one of the most active base metal catalysts for the hydrogenation of unactivated, sterically hindered olefins such as *trans*-methylstilbene, 1-methyl-1-cyclohexene and 2,3-dimethyl-2-butene. Spectroscopic observation of the catalytically relevant hydride compound, (^{iPr}CNC)CoH established hydride migration to the 4-position of the pyridine ring of the chelate. This reactivity was extended to alkyls upon addition of 1,1-diphenylethylene to (^{iPr}CNC)CoH. The chemical participation of the ligand signaled the possibility of ligand radicals in the electronic structure of (^{iPr}CNC)CoX (X = halide, alkyl, H) compounds. Accordingly, a combination of structural, spectroscopic and computational studies established bis(arylimidazol-2-ylidene)pyridine chelates as redox-active, undergoing one electron reduction in reduced cobalt chemistry. Unlike redox-active bis(imino)pyridines which have a more extended π system, the ligand-centered radical in the bis(arylimidazol-2-ylidene)pyridine is essentially pyridine localized, likely contributing to the observed hydride and alkyl migration chemistry. These studies establish the utility of bis(arylimidazol-2-ylidene)pyridines as excellent support ligands in base metal catalysis and also adds these pincers to the growing number of examples of redox-active tridentate chelates.[82] These results also suggest that other pyridine-based pincer ligands may be redox-active when coordinated to an appropriately reducing bas metal. This question and its broader impact on base metal catalysis are currently under scrutiny in our laboratory.

Experimental Section[83]

Preparation of (4-CPh_2CH_3-^{iPr}CNC)CoN_2

A thick-walled glass vessel was charged with 0.100 g (0.160 mmol) of (^{iPr}CNC)$CoCH_3$ and approximately 10 mL of toluene. The vessel was submerged in a -78 °C bath and the headspace was evacuated and replaced with an atmosphere of H_2. The contents of the vessel were warmed to ambient temperature and stirred for 15 minutes. The excess dihydrogen was removed at −78 °C and 0.030 g (0.170 mmol) of 1,1-diphenylethylene was added at 22 °C under an atmosphere of dinitrogen. A rapid color change to deep blue was observed and the reaction mixture was stirred for an additional 15 minutes. The solution was then filtered through Celite and concentrated to dryness. The residue was dissolved in diethyl ether and stored at −35 °C to afford 0.082 g (0.010 mmol, 62% yield) of blue solid identified as (4-CPh_2CH_3-^{iPr}CNC)CoN_2. Analysis for $C_{49}H_{54}N_7Co$: Calc. C, 73.57; H, 6.80; N, 12.26. Found: C, 73.52; H, 6.66; N, 11.93. ^{1}H NMR (benzene-d_6, 22 °C): δ = 0.99 (d, 7 Hz, 6H, $CH(CH_3)_2$), 1.03 (d, 7 Hz, 6H, $CH(CH_3)_2$), 1.37 (d, 7 Hz, 12H, $CH(CH_3)_2$), 1. 77 (s, 3H, Ph_2CCH_3), 2.87 (spt, 7 Hz, 2H, $CH(CH_3)_2$), 2.91 (spt, 7 Hz, 2H, $CH(CH_3)_2$), 4.33 (d, 4 Hz, 2H, *vinyl H*), 4.90 (t, 4 Hz, 1H, *allyl H*), 6.03 (d, 2 Hz, 2H, *imidazolylidene backbone*), 6.30

(d, 2 Hz, 2H, *imidazolylidene backbone*), 6.96 (d, 7 Hz, 4H, *aryl* or *phenyl*), 7.06 (t, 7 Hz, 4H, *aryl* or *phenyl*), 7.18 (d, 7 Hz, 4H, *aryl* or *phenyl*), 7.35 (d, 7 Hz, 4H, *aryl* or *phenyl*). ^{13}C {^{1}H} NMR (benzene-d_6, 22 °C): δ = 22.4 (Ph_2CCH_3), 23.9 ($CH(CH_3)_2$), 24.0 ($CH(CH_3)_2$), 24.4 ($CH(CH_3)_2$), 24.5 ($CH(CH_3)_2$), 28.5 ($CH(CH_3)_2$), 28.6 ($CH(CH_3)_2$), 45.2 (allyl), 53.1 (Ph_2CCH_3), 77.5 (vinyl), 113.3 (*imidazolylidene backbone*), 123.0 (*imidazolylidene backbone*), 123.7 (*aryl*), 123.8 (*phenyl*), 125.6 (*aryl*), 128.3 (*phenyl*), 129.8 (*phenyl*), 136.0 (*aryl*), 145.9 (*aryl* or 2-*pyr*), 146.23 (*aryl* or 2-*pyr*), 146.25 (*aryl* or 2-*pyr*), 149.0 (*phenyl*), 194.1 (*carbene*), one resonance not located. IR (benzene-d_6, 22 °C): $\nu(N_2)$ = 2050 cm^{-1}

Preparation of [(^{iPr}CNC)CoCH$_3$][BAr$^F_4$] (BAr$^F_4$ = B(3,5-(CF$_3$)$_2$C$_6$H$_3$)$_4$)

A 20 mL scintillation vial equipped with a magnetic stir bar was charged with (^{iPr}CNC)CoCH$_3$ (0.036 g, 0.059 mmol, 1 equiv.) and approximately 2 mL of fluorobenzene. The solution was chilled in a -35 °C freezer for 10 minutes, then a diethyl ether solution of [Cp_2Fe][BAr$^F_4$] (0.062 g, 0.059 mmol, 1 equiv., in 1 mL diethyl ether) was added dropwise with rapid magnetic stirring. An immediate color change from yellowish-brown to blue-green was observed. The mixture was stirred at 22 °C for 5 minutes, after which the mixture was filtered through Celite and subsequently stored at −15 °C. Over a period of 2 hours, a brown-colored oil condensed on the bottom of the glass container and was separated from the supernatant by carefully decanting the solution into a clean 20-mL scintillation vial. After 3 repeated decanting processes over a period of 6 hours, the solution eventually resumed a teal color, with no further formation of a brown oil. Layering the solution with pentane (~ 5 mL) and storing the mixture at −15 °C resulted formation of bright green crystals identified as [(^{ipr}CNC)CoCH$_3$][BAr$^F_4$] (0.013 g, 0.009 mmol, 15% yield). Once crystalline, the solid was no longer soluble in benzene, toluene or light hydrocarbons but was highly soluble in diethyl ether and fluorobenzene. Analysis for $C_{68}H_{56}BCoF_{24}N_5$: Calc. C, 55.60; H, 3.82; N, 4.77. Found: C, 55.45; H, 4.11; N, 4.49. μ_{eff} (Evans method, 22 °C) = 1.8(5) μ_B. ^1H NMR (benzene-d_6, 22 °C): δ = -9.98 (182 Hz, 12H, $CH(CH_3)_2$), 4.39 (22 Hz, 12H, $CH(CH_3)_2$), 6.57 (12 Hz, 4H, *m*-BAr$^F_4$), 7.85 (9 Hz, 10H, *o*-BAr$^F_4$ and *p-aryl)*, 8.84 (20 Hz, 4H, $CH(CH_3)_2$), 9.35 (17 Hz, 2H, *3-pyr)*, 12.64 (474 Hz, 3H, $CoCH_3$), 15.61 (76 Hz, 2H, *imidazolylidene backbone)*, 16.07 (94 Hz, 2H, *imidazolylidene backbone)*, 26.25 (33 Hz, 1H, 4-*pyr), m-aryl* not located.

Supplementary Material

Refer to Web version on PubMed Central for supplementary material.

Acknowledgments

PJC thanks the U. S. National Science Foundation and Deutsche Forschungsgemeinschaft for a Cooperative Activities in Chemistry between U. S. and German Investigators grant (CHE-1026084). JMD also acknowledges support from the National Institute of General Medical Sciences (Award Number T32GM008500). SCES thanks NSF for a graduate research fellowship (DGE-0646086) for support. Portions of the research were carried out at the Stanford Synchrotron Radiation Lightsource, a national user facility operated by Stanford University on behalf of the DOE, BES. The SSRL SMB Program is supported by DOE, BER and NIH, NCRR, BMTP. The simulations presented in this article were performed on computational resources supported by the Princeton Institute for Computational Science and Engineering (PICSciE) and the Office of Information Technology's High Performance Computing Center and Visualization Laboratory at Princeton University. We also thank Scott Semproni for assistance with X-ray diffraction.

References

1. Hartwig, J. Organotransition Metal Chemistry: From Bonding to Catalysis. University Science Books; Sausalito, California: 2010. p. 575

2. (a) Chirik PJ, Wieghardt K. Science. 2010; 327:794. [PubMed: 20150476] (b) Enthaler S, Junge K, Beller M. Angew Chem Int Ed. 2008; 47:3317.(c) Nakazawa H, Itazaki M. Top Organomet Chem. 2011; 33:27.(d) Junge K, Schröder K, Beller M. Chem Commun. 2011; 47:4849.
3. (a) Bolm C, Legros J, Paith JL, Zani L. Chem Rev. 2004; 104:6217. [PubMed: 15584700] (b) Bauer EB. Curr Org Chem. 2008; 47:1341.(c) Gaillard S, Renaud JL. ChemSusChem. 2008; 1:505. [PubMed: 18702146] (d) Chirik, PJ. Catalysis Without Precious Metals. Bullock, RM., editor. Vol. Chapter 4. Wiley-VCH; Weinheim: 2010.
4. Crabtree, RH. The Organometallic Chemistry of the Transition Metals. 4th. John Wiley & Sons; New York: 2005.
5. (a) DeAngelis F, Jin N, Car R, Groves JT. Inorg Chem. 2006; 45:4268. [PubMed: 16676990] (b) Dhuri SN, Seo MS, Lee YM, Hirao H, Wang Y, Nam W, Shaik S. Angew Chem Int Ed. 2008; 47:3356.(c) Klinker EJ, Shaik S, Hirao H, Que L. Angew Chem Int Ed. 2009; 48:1291.
6. Volpe EC, Wolczanski PT, Lobkovsky EB. Organometallics. 2010; 29:364.
7. (a) Frankel EN, Emken EA, Peters HM, Davison VK, Butterfield RO. J Org Chem. 1964; 29:3292. (b) Frankel EN, Emken EA, Davison VK. J Org Chem. 1965; 30:2739.(c) Wrighton M. Chem Rev. 1974; 74:401.(d) Schroeder MA, Wrighton MS. J Am Chem Soc. 1976; 98:551.(e) Mitchener JC, Wrighton MS. J Am Chem Soc. 1981; 103:975.(f) Wuu YM, Bentsen JG, Brinkley CG, Wrighton MS. Inorg Chem. 1987; 26:530.
8. (a) Das S, Li YH, Junge K, Beller M. Chem Comm. 2012; 48:10742. [PubMed: 23024977] (b) Fleisher S, Zhou SL, Junge K, Beller M. Chem Asian J. 2011; 6:2240. [PubMed: 21793223] (c) Gartner F, Boddien A, Barsch E, Fumino K, Losse S, Junge H, Hollmann D, Bruckner A, Ludwig R, Beller M. Chem Eur J. 2011; 17:6425. [PubMed: 21506181] (d) Boddien A, Loges B, Gartner F, Torborg C, Fumino K, Junge H, Ludwig R, Beller M. J Am Chem Soc. 2010; 132:8294.(e) Zhou SL, Addis D, Das S, Junge K, Beller M. Chem Commun. 2009; 32:4883.(f) Shaikh NS, Enthaler S, Junge K, Beller M. Angew Chem Int Ed. 2008; 47:2497.
9. (a) Jørgensen CK. Coord Chem Rev. 1966; 1:164.(b) Pierpont CG. Coord Chem Rev. 2001; 216:99. (c) Evangelio E, Ruiz-Molina D. Eur J Inorg Chem. 2005:2957.(d) Ray K, Petrenko T, Wieghardt K, Neese F. Dalton Trans. 2007:1552. [PubMed: 17426855] (e) De Bruin B, Hetterscheid DGH, Koekkoek AJJ, Grutzmacher H. Prog Inorg Chem. 2007; 55:247–354.
10. Chirik PJ. Inorg Chem. 2011; 50:9737. [PubMed: 21894966]
11. Luca OR, Crabtree RH. Chem Soc Rev. 2012; 42:1440. [PubMed: 22975722]
12. Darmon JM, Stieber SCE, Sylvester K, Fernandez I, Lobkovsky E, Semproni SP, Bill E, Wieghardt K, DeBeer S, Chirik PJ. J Am Chem Soc. 2012; 134:17125. [PubMed: 23043331]
13. (a) Stubbe J, Van der Donk WA. Chem Rev. 1998; 98:706.(b) Jazdewski BA, Tolman WB. Coord Chem Rev. 2000; 633:200–202.(c) Lewis EA, Tolman WB. Chem Rev. 2004; 104:1047. [PubMed: 14871149] (d) Kaim W, Schwederski B. Coord Chem Rev. 2010; 254:1580.(e) Rittle J, Green MT. Science. 2010; 330:933. [PubMed: 21071661]
14. Lyaskovsky V, de Bruin B. ACS Catalysis. 2012; 2:270.
15. Praneeth VKK, Ringenberg MR, Ward TR. Angew Chem Int Ed. 2012; 51:10228.
16. (a) Heyduk AF, Zarkesh RA, Nguyen AI. Inorg Chem. 2011; 50:9849. [PubMed: 21774482] (b) Nguyen N, Zarkesh RA, Lacy DC, Thorson MK, Heyduk AF. Chem Sci. 2011; 2:166.(c) Zarkesh RA, Ziller JW, Heyduk AF. Angew Chem Int Ed. 2008; 47:4715.(d) King ER, Hennessy ET, Betley TA. J Am Chem Soc. 2011; 133:4917. [PubMed: 21405138]
17. (a) Lippert CA, Riener K, Soper JD. Eur J Inorg Chem. 2012:554.(b) Lippert CA, Hardcastle KI, Soper JD. Inorg Chem. 2011; 50:9864. [PubMed: 21744815] (c) Smith AL, Hardcastle KI, Soper JD. J Am Chem Soc. 2010; 132:14358. [PubMed: 20879770] (d) Lippert CA, Soper JD. Inorg Chem. 2010; 49:3682. [PubMed: 20334351]
18. Bart SC, Lobkovsky E, Chirik PJ. J Am Chem Soc. 2004; 126:13794. [PubMed: 15493939]
19. (a) Russell SK, Darmon JM, Lobkovsky E, Chirik PJ. Inorg Chem. 2010; 49:2782. [PubMed: 20143847] (b) Archer AM, Bouwkamp MW, Cortez MP, Lobkovsky E, Chirik PJ. Organometallics. 2006; 25:4269.(c) Trovitch RJ, Lobkovsky E, Bouwkamp MW, Chirik PJ. Organometallics. 2008; 27:6264.(d) Trovitch RJ, Lobkovsky E, Bill E, Chirik PJ. Organometallics. 2008; 27:1470.

20. (a) Tondreau AM, Atienza CCH, Weller KJ, Nye SA, Lewis KM, Delis JGP, Chirik PJ. Science. 2012; 335:567. [PubMed: 22301315] (b) Atienza CCH, Tondreau AM, Turner ZR, Weller KJ, Lewis KM, Cruse RW, Nye SA, Boyer JL, Delis JGP, Chirik PJ. ACS Catal. 2012; 2:2169.
21. For an additional examples of iron-catalyzed hydrosilylation see:(a) Kamata K, Suzuki A, Nakai Y, Nakazawa H. Organometallics. 2012; 31:3825.(b) Tondreau AM, Atienza CCH, Darmon JM, Milsmann C, Hoyt HM, Weller KJ, Nye SA, Lewis KM, Boyer J, Delis JGP, Lobkovsky E, Chirik PJ. Organometallics. 2012; 31:4886.(c) Naumov RN, Itazaki M, Kamitani M, Nakazawa H. J Am Chem Soc. 2012; 134:804. [PubMed: 22206470] (d) Wu JY, Stanzi BN, Ritter T. J Am Chem Soc. 2010; 132:13214. [PubMed: 20809631]
22. Bouwkamp MW, Bowman AC, Lobkovsky E, Chirik PJ. J Am Chem Soc. 2006; 128:13340. [PubMed: 17031930]
23. Russell SK, Lobkovsky E, Chirik PJ. J Am Chem Soc. 2011; 133:8858. [PubMed: 21598972]
24. Hoyt JM, Sylvester KT, Semproni SP, Chirik PJ. J Am Chem Soc. 2013; 135:4862. [PubMed: 23448301]
25. Obligacion JV, Chirik PJ. Org Lett. 2013; 15:2680. [PubMed: 23688021]
26. For other examples of iron-catalyzed hydroboration see:(a) Zhang L, Peng DJ, Leng XB, Huang Z. Angew Chem Int Ed. 2013; 52:3676.(b) Wu JY, Moreau B, Ritter T. J Am Chem Soc. 2009; 131:12915. [PubMed: 19702262]
27. Blanchard S, Derat E, Desage-El Murr M, Fensterbank MalacriaM, Mouriès-Mansuy V. Eur J Inorg Chem. 2012:376.
28. Yu RP, Darmon JM, Hoyt JM, Margulieux GW, Turner ZR, Chirik PJ. ACS Catal. 2012; 2:1760.
29. Darmon JM, Turner ZR, Lobkovsky E, Chirik PJ. Organometallics. 2012; 31:2275. [PubMed: 22675236]
30. Danopoulos AA, Wright JA, Motherwell WB. Chem Commun. 2005:784.
31. Roseblade SJ, Pfaltz A. Acc Chem Res. 2007; 40:1402. [PubMed: 17672517]
32. (a) Leutenegger U, Madin A, Pflatz A. Angew Chem Int Ed Engl. 1989:60.(b) Nindakova LO, Lebed FM, Shainyan BA. Russ J Org Chem. 2007; 43:1332.(c) Inagaki T, Phong LT, Furuta A, Ito J, Nishiyama H. Chem Eur J. 2010; 16:3090. [PubMed: 20119993] (d) Yu F, Zhang XC, Wu FF, Zhou JN, Fang W, Wu J, Chan ASC. Org Biomol Chem. 2011; 9:5652. [PubMed: 21709901] (e) Corma A, Iglesias M, del Pino C, Sánchez F. J Organomet Chem. 1992; 431:233.(f) DuBois DL, Meek DW. Inorg Chim Acta. 1976; 19:L29.(g) Ohgo Y, Takeuchi S, Natori Y, Yoshimura J. Bull Chem Soc Jpn. 1981; 54:2124.(h) Takeuchi S, Ohgo Y. Bull Chem Soc Jpn. 1987; 60:1449.
33. Kooistra TM, Knijnenburg Q, Smits JMM, Horton AD, Budzelaar PHM, Gal AW. Angew Chem Int Ed. 2001; 40:4719.
34. Gibson VC, Humphries MJ, Tellmann KP, Wass DF, White AJP, Williams DJ. Chem Commun. 2001:2252.
35. Knijnenburg Q, Horton AD, van der Heijden H, Kooistra TM, Hetterscheid DGH, Smits JMM, de Bruin B, Budzelaar PHM, Gal AW. J Mol Cat -A. 2005; 232:151.
36. Monfette S, Turner ZR, Semproni SP, Chirik PJ. J Am Chem Soc. 2012; 134:4561. [PubMed: 22390262]
37. Zhang G, Scott BL, Hanson SK. Angew Chem Int Ed. 2012; 51:12102.
38. Zhang G, Hanson SK. Org Lett. 2013; 15:650. [PubMed: 23311959]
39. Zhang G, Vasudevan KV, Scott BL, Hanson SK. J Am Chem Soc. 2013; 135:8668. [PubMed: 23713752]
40. Danopoulos AA, Wright JA, Motherwell WB, Ellwood S. Organometallics. 2004; 23:4807.
41. (a) Roseblade SJ, Pfaltz A. Acc Chem Res. 2007; 40:1402. [PubMed: 17672517] (b) Broene RD, Buchwald SL. J Am Chem Soc. 1993; 115:12569.(c) Troutman MV, Appella DH, Buchwald SL. J Am Chem Soc. 1999; 121:4916.
42. Cámpora J, Perez CM, Rodriguez-Delgado A, Naz AM, Palma P, Alvarez E. Organometallics. 2007; 26:1104.
43. Jiao Y, Evans ME, Morris J, Brennessel WW, Jones WD. J Am Chem Soc. 2013; 135:6994. [PubMed: 23611483]

44. Hounjet LJ, Bannwarth C, Garon CN, Caputo CB, Grimme S, Stephan DW. Angew Chem Int Ed. 2013; 52:7492.
45. Hartung, J.; Norton, JR. Catalysis without Precious Metals. Bullock, RM., editor. Vol. Chapter 1. Wiley-VCH; Weinheim: 2010.
46. (a) Feder HM, Halpern JJ. Am Chem Soc. 1975; 97:7186.(b) Weil TA, Friedman S, Wender I. J Org Chem. 1974; 39:48.
47. Sweany RL, Halpern J. J Am Chem Soc. 1977; 99:8335.
48. Tang L, Papish ET, Abramo GP, Norton JR, Baik MH, Friesner RA, Rappé A. J Am Chem Soc. 2003; 125:10093. [PubMed: 12914473]
49. Tang L, Papish ET, Abramo GP, Norton JR, Baik MH, Friesner RA, Rappé A. J Am Chem Soc. 2006; 128:11314.
50. Bullock RM, Samsel EG. J Am Chem Soc. 1990; 112:6886.
51. Choi J, Pulling ME, Smith DM, Norton JR. J Am Chem Soc. 2008; 130:4250. [PubMed: 18335937]
52. Knijnenburg Q, Hetterscheid D, Kooistra TM, Budzelaar PHM. Eur J Inorg Chem. 2004:1204.
53. Tondreau AM, Darmon JM, Wile BM, Floyd SK, Lobkovsky E, Chirik PJ. Organometallics. 2009; 28:2928.
54. Darmon JM, Turner ZR, Lobkovsky E, Chirik PJ. Organometallics. 2012; 31:2275. [PubMed: 22675236]
55. For early electrochemical studies identifying the redox-activity of bis(imino)pyridines see:(a) Kuwabara IH, Comninos FCM, Pardini VL, Viertler H, Toma HE. Electrochim Acta. 1994; 39:2401.(b) Toma HE, Chavez-Gil TE. Inorg Chim Acta. 1997; 257:197.(c) de Bruin B, Bill E, Bothe E, Weyhermüller T, Wieghardt K. Inorg Chem. 2000; 39:2936. [PubMed: 11232835] (d) Budzelaar PHM, de Bruin B, Gal AW, Wieghardt KW, van Lenthe JH. Inorg Chem. 2001; 40:4649. [PubMed: 11511211]
56. Danopoulos AA, Winston S, Motherwell WB. Chem Commun. 2002:1376.
57. Britovsek GJP, Clentsmith GKB, Gibson VC, Goodgame DML, McTavish SJ, Pankhurst QA. Catal Commun. 2002; 3:207.
58. Scott J, Gambarotta S, Korobkov I, Knijnenburg Q, de Bruin B, Budzelaar PHM. J Am Chem Soc. 2005; 127:17204. [PubMed: 16332066]
59. Milsmann C, Turner ZR, Semproni SP, Chirik PJ. Angew Chem Int Ed. 2012; 51:5386.
60. Bowman AC, Milsmann C, Atienza CCH, Lobkovsky E, Wieghardt K, Chirik PJJ. Am Chem Soc. 2010; 132:1676.
61. Talcott CL, Myers R. J Molecular Physics. 1967; 12:549.
62. Danopoulos AA, Tulloch AAD, Winston S, Eastham G, Hursthouse MB. Dalton Trans. 2003:1009.
63. Bogdanovic B. Acc Chem Res. 1988; 21:261.
64. Bowman AC, Milsmann C, Bill E, Lobkovsky E, Weyhermüller T, Wieghardt K, Chirik PJ. Inorg Chem. 2010; 49:6110. [PubMed: 20540554]
65. Atienza CCH, Milsmann C, Lobkovsky E, Chirik PJ. Angew Chem Int Ed. 2011; 50:8143.
66. (a) Maki AH, Edelstein N, Davison A, Holm RHJ. Am Chem Soc. 1964; 86:4580.(b) Nishida Y, Hayashida K, Sumita A, Kida S. Bull Chem Soc Jpn. 1980; 53:271.(c) Nishida Y, Kida S. Bull Chem Soc Jpn. 1978; 51:143.(d) Matsuzaki K, Yasukawa T. Chem Commun. 1968:1460.(e) Nishida Y, Sumita A, Kida S. Bull Chem Soc Jpn. 1977; 50:759.(f) Przyojski JA, Arman HD, Tonzetich ZJ. Organometallics. 2013; 32:723.(g) Gregson AK, Martin RL, Mitra S. Chem Phys Lett. 1970; 5:310.(h) Mo Z, Li Y, Lee HK, Deng L. Organometallics. 2011; 30:4687.(H) Hay-Motherwell RS, Wilkinson G, Hussain B, Hursthouse MB. Polyhedron. 1990; 9:931.
67. (a) Pierpont CG, Lange CW. Prog Inorg Chem. 1994; 41:331.(b) Ray K, Petrenko T, Wieghardt K, Neese F. Dalton Trans. 2007:1552. [PubMed: 17426855]
68. Knijnenburg Q, Gambarotta S, Budzelaar PHM. Dalton Trans. 2006; 46:5542.
69. (a) Tomson NC, Crimmin MR, Petrenko T, Rosebrugh LE, Sproules S, Boyd WC, Bergman RG, DeBeer S, Toste FD, Wieghardt K. J Am Chem Soc. 2011; 133:18785. [PubMed: 22047035] (b) Sarangi R, Cho J, Nam W, Solomon EI. Inorg Chem. 2011; 50:614.

70. Stieber SCE, Milsmann C, Hoyt JM, Turner ZR, Finkelstein KD, Weighardt K, Debeer S, Chirik PJ. Inorg Chem. 2012; 51:3770. [PubMed: 22394054]
71. Bowman AC, Milsmann C, Bill E, Turner ZR, Lobkovsky E, DeBeer S, Wieghardt K, Chirik PJ. J Am Chem Soc. 2011; 133:17353. [PubMed: 21985461]
72. Westre TE, Kennepohl P, DeWitt JG, Hedman B, Hodgson KO, Solomon EI. J Am Chem Soc. 1997; 119:6297.
73. Chandrasekaran P, Stieber SCE, Collins TJ, Que L, Neese F, DeBeer S. Dalton Trans. 2011; 40:11070. [PubMed: 21956429]
74. Zhu D, Thapa I, Korobkov I, Gambarotta S, Budzelaar PHM. Inorg Chem. 2011; 50:9879. [PubMed: 21520927]
75. Bart SC, Chlopek K, Bill E, Bouwkamp MW, Lobkovsky E, Neese F, Wieghardt K, Chirik PJ. J Am Chem Soc. 2006; 128:13901. [PubMed: 17044718]
76. Humphries MJ, Tellmann KP, Gibson VC, White AJP, Williams DJ. Organometallics. 2005; 24:2039.
77. Bart SC, Lobkovsky E, Bill E, Wieghardt K, Chirik PJ. Inorg Chem. 2007; 46:7055. [PubMed: 17655227]
78. Noodleman L, Peng CY, Case DA, Mouesca JM. Coord Chem Rev. 1995; 144:199.
79. Ginsberg AP. J Am Chem Soc. 1980; 102:111.
80. Kirchner B, Wennmohs F, Ye S, Neese F. Curr Opin Chem Biol. 2007; 11:134. [PubMed: 17349817]
81. (a) DeBeer, GeorgeS; Petrenko, T.; Neese, F. J Phys Chem A. 2008; 112:12936. [PubMed: 18698746] (b) Chandrasekaran P, Stieber SCE, Collins TJ, Que L, Neese F, DeBeer S. Dalton Trans. 2011; 40:11070. [PubMed: 21956429]
82. Caulton KG. Eur J Inorg Chem. 2012:435.
83. Only representative procedures are reported here. Full experimental details, including General Considerations, are reported in the Supporting Information.

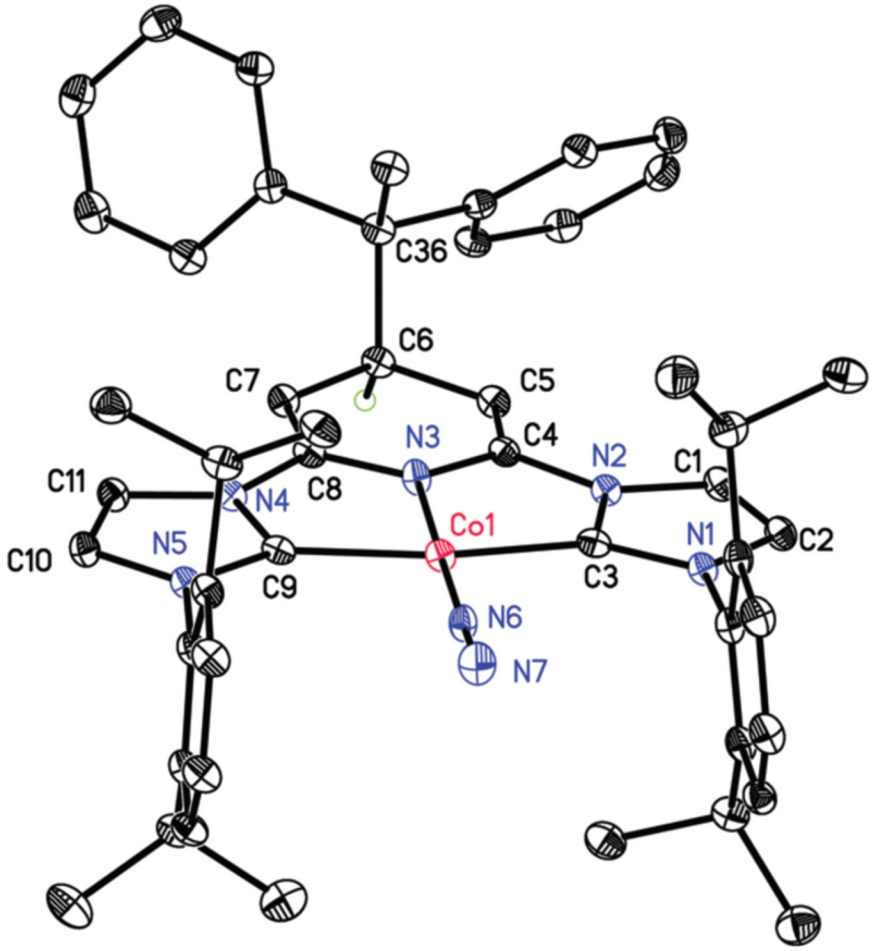

Figure 1.

Solid state molecular structure of (4-CPh_2CH_3-^{iPr}CNC)CoN_2 at 30% probability ellipsoids. Hydrogen atoms, except for the one attached to C(6), and one diethyl ether molecule were omitted for clarity.

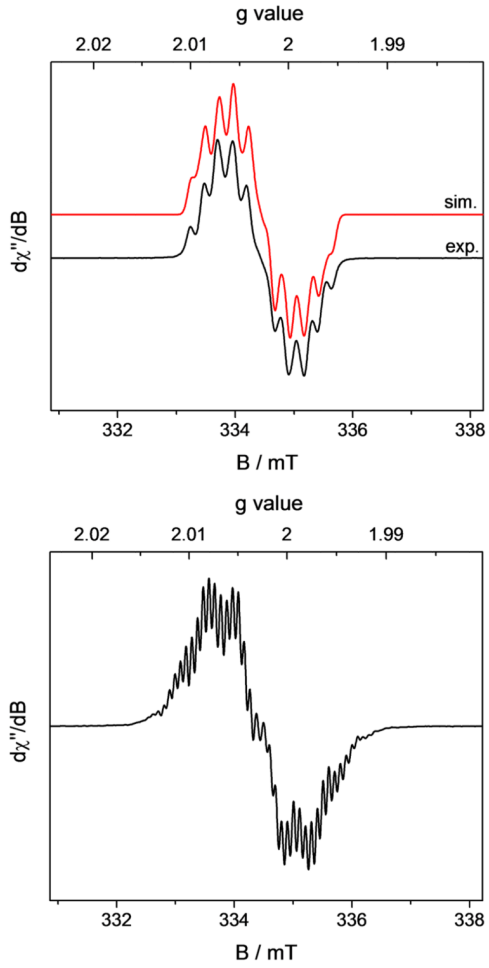

Figure 2.

THF/Toluene solution EPR spectrum of Na[(^{iPr}BPDI)] (top) and Na[^{iPr}PDI] (bottom) recorded at 298 K. Conditions for (a) Na[(^{iPr}BPDI)]: microwave frequency = 9.3749 GHz, power = 0.63 mW, modulation amplitude = 0.05 mT/100 kHz; (b) Na[(^{iPr}PDI)]: microwave frequency = 9.3746 GHz, power = 0.63 mW, modulation amplitude = 0.05 mT/100 kHz.

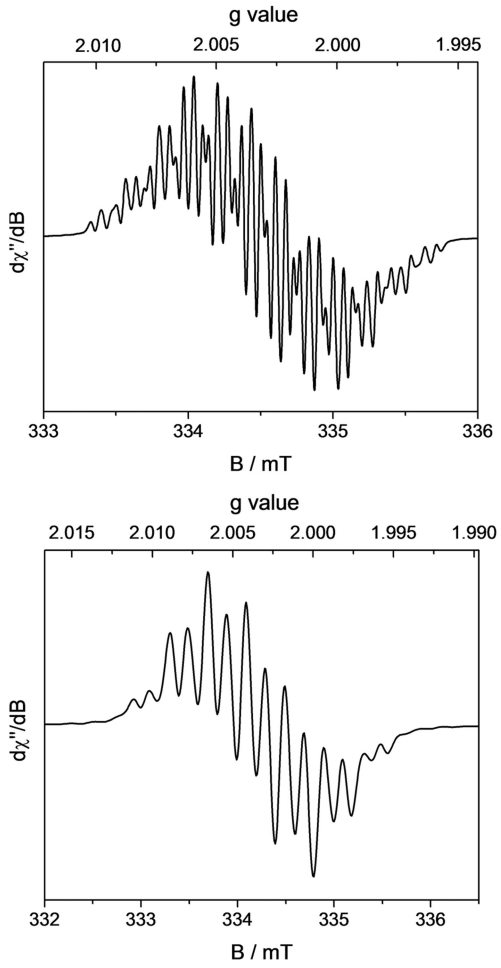

Figure 3.

Toluene solution EPR spectrum of Na[^{iPr}CNC] (top) and MgBr[(^{iPr}CNC)] (bottom) recorded at 298 K. Conditions for (a) Na[^{iPr}CNC]: microwave frequency = 9.3783 GHz, power = 2.00 mW, modulation amplitude = 0.02 mT/100 kHz; (b) MgBr[(^{iPr}CNC)]: microwave frequency = 9.3710 GHz, power = 2.00 mW, modulation amplitude = 0.1 mT/ 100 kHz.

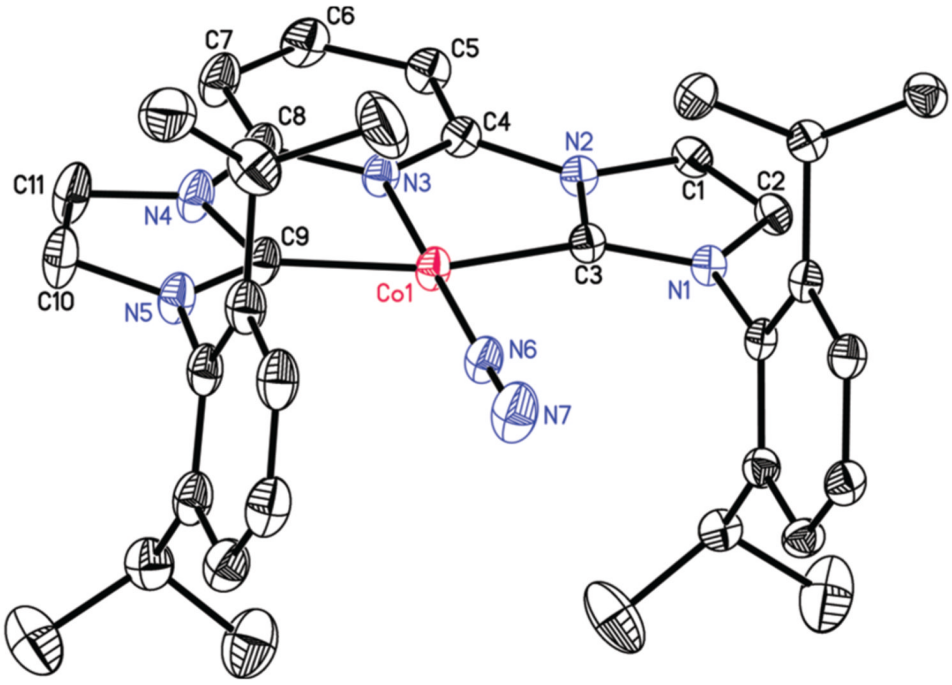

Figure 4.
Solid state molecular structure of [(^{iPr}CNC)CoN$_2$][BAr$^F_4$] at 30% probability ellipsoids. Hydrogen atoms, one molecule of pentane and BAr$^F_4$ anion were omitted for clarity. See Supporting Information for full structural representation.

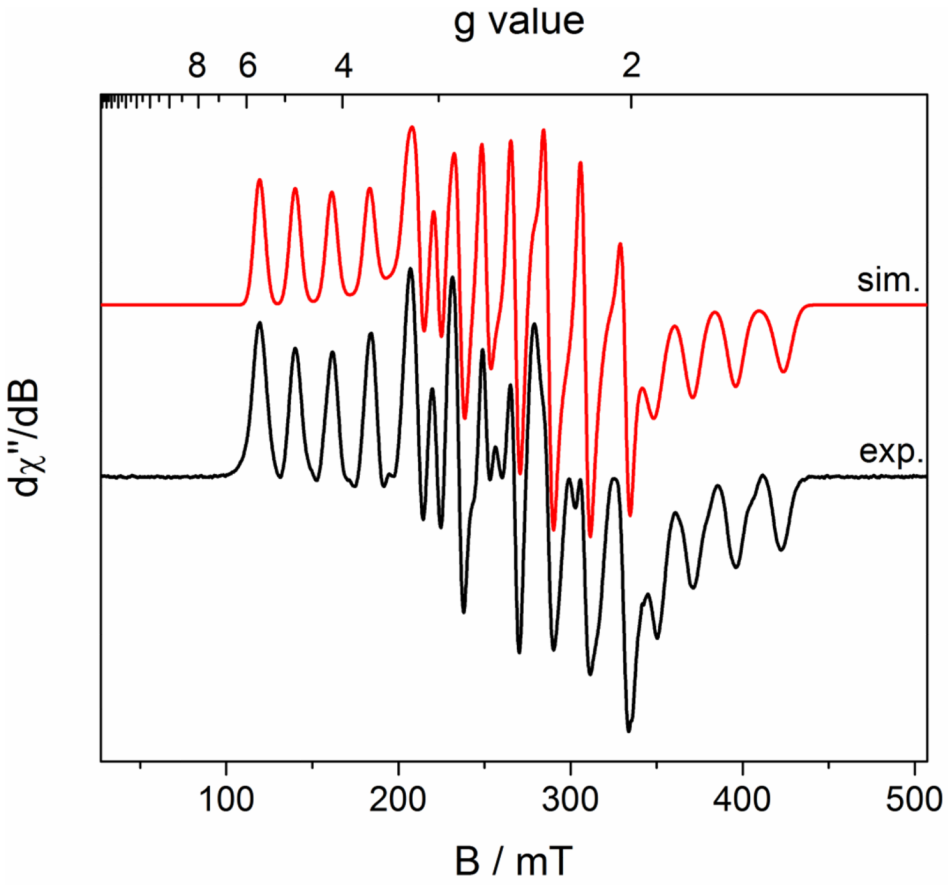

Figure 5.
Solid state powder EPR spectrum of [(^{iPr}CNC)CoCH$_3$][BAr$^F_4$] recorded at 10 K. Conditions: microwave frequency = 9.3825 GHz, power = 0.5 mW, modulation amplitude = 1.0 mT/100 kHz;

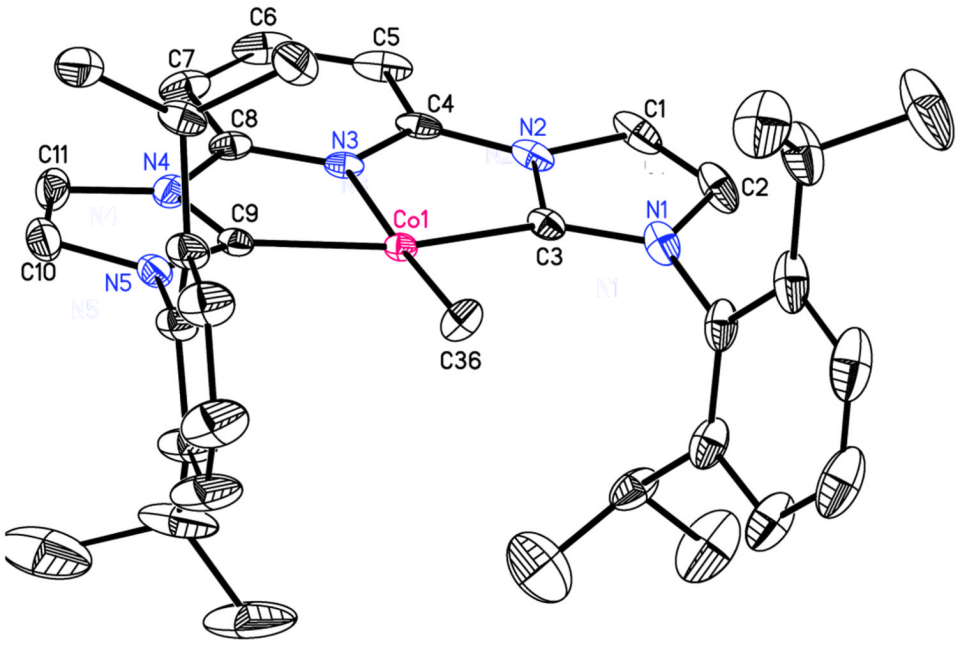

Figure 6.
Solid state molecular structure of [(^{iPr}CNC)CoCH$_3$][BAr$^F_4$] at 30% probability ellipsoids. Hydrogen atoms and BAr$^F_4$ anion were omitted for clarity. See Supporting Information for full structure representation.

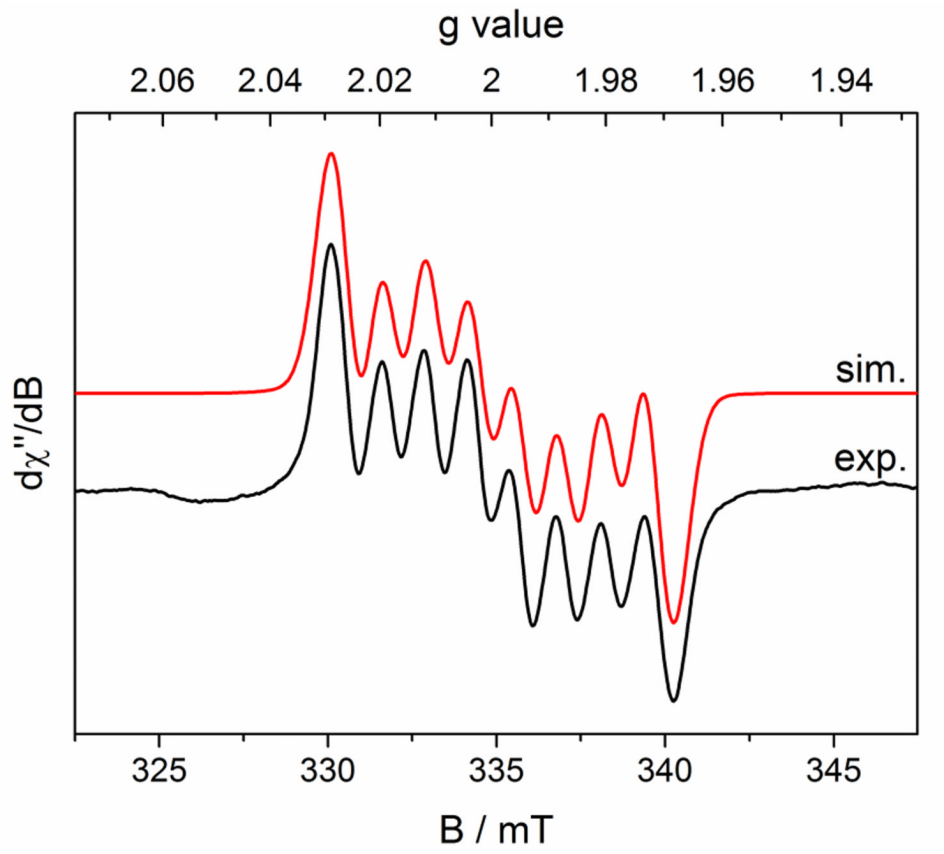

Figure 7.

Benzene solution EPR spectrum of (^{iPr}CNC)CoN_2 recorded at 298 K. Conditions: microwave frequency = 9.3735 GHz, power = 20.0 mW, modulation amplitude = 0.10 mT/ 100 KHz. Simulation was performed with the presence of an unidentified $S = 1/2$ species at $g = 2.000$. The relative ratio of (^{iPr}CNC)CoN_2 and the unidentified species in this spectrum is approximately 3:2. See Supporting Information for subspectra from the simulation and decomposition time course.

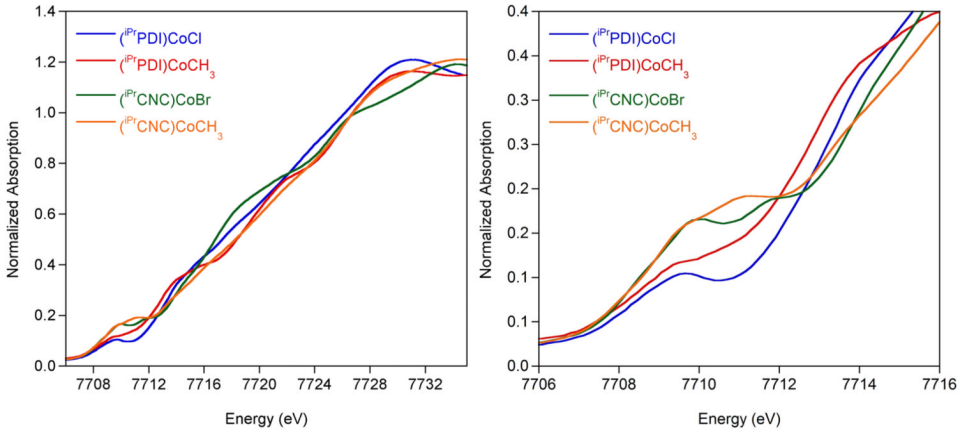

Figure 8.

Normalized Co K-edge X-ray absorption spectra of the rising edge (left) and pre-edge (right) of (^{iPr}CNC)CoBr and (^{iPr}CNC)CoCH$_3$ recorded at 10 K. Also included are the data for (^{iPr}PDI)CoCl and (^{iPr}PDI)CoCH$_3$.

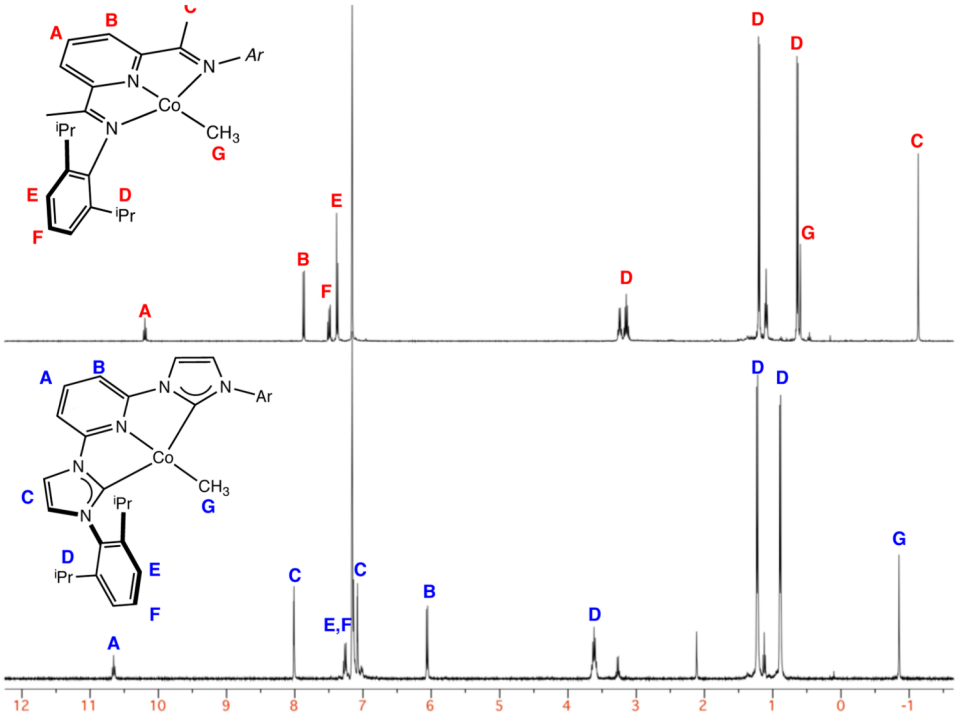

Figure 9.
Benzene-d_6 ^{1}H NMR spectra of (^{iPr}PDI)CoCH$_3$ (top) and (^{iPr}CNC)CoCH$_3$ (bottom). The data for (^{iPr}PDI)CoCH$_3$ was previously reported in ref. 76 and (^{iPr}CNC)CoCH$_3$ in ref. 40.

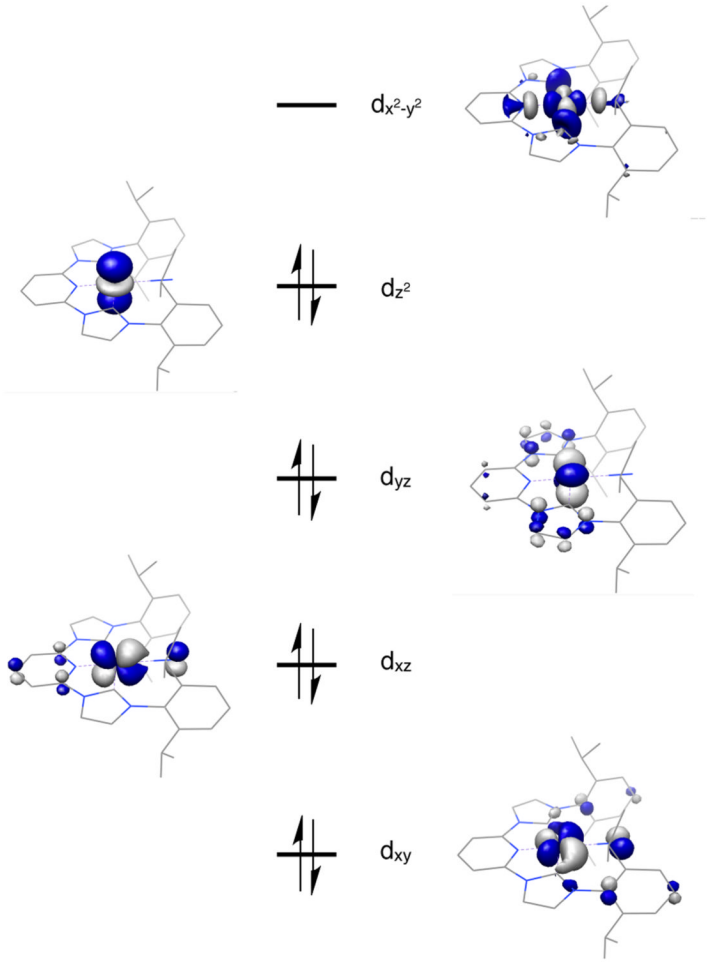

Figure 10.
Qualitative molecular orbital diagram for $[(^{iPr}PDICoN_2]^+$ from a geometry optimized B3LYP calculation.

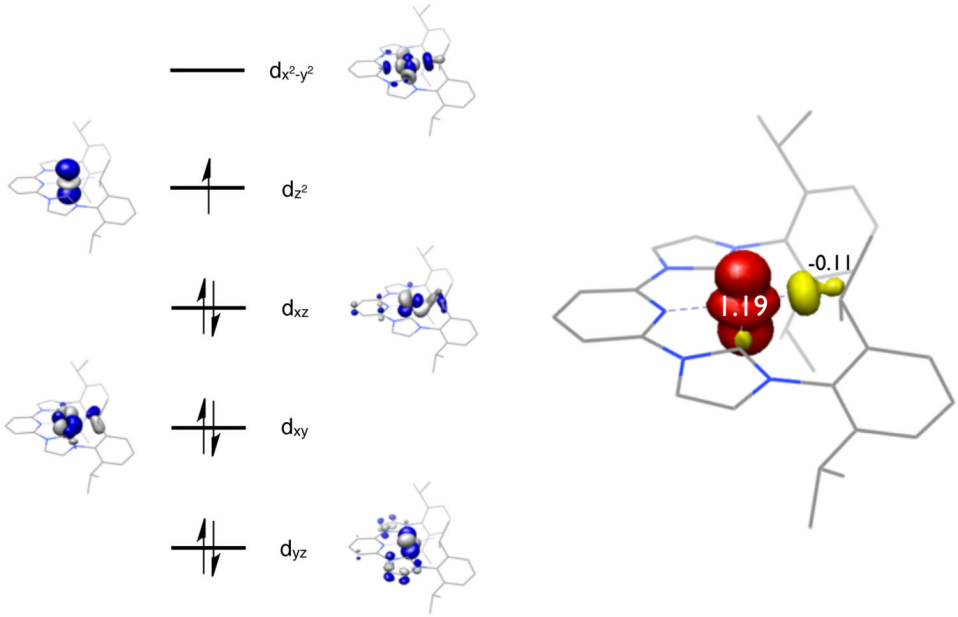

Figure 11.

Qualitative molecular orbital diagram (left) for [(^{iPr}CNC)CoCH$_3$]$^+$ from an UKS calculation at B3LYP level. Spin density plot (right) was obtained from Mulliken population analysis (red, positive spin density; yellow, negative spin density).

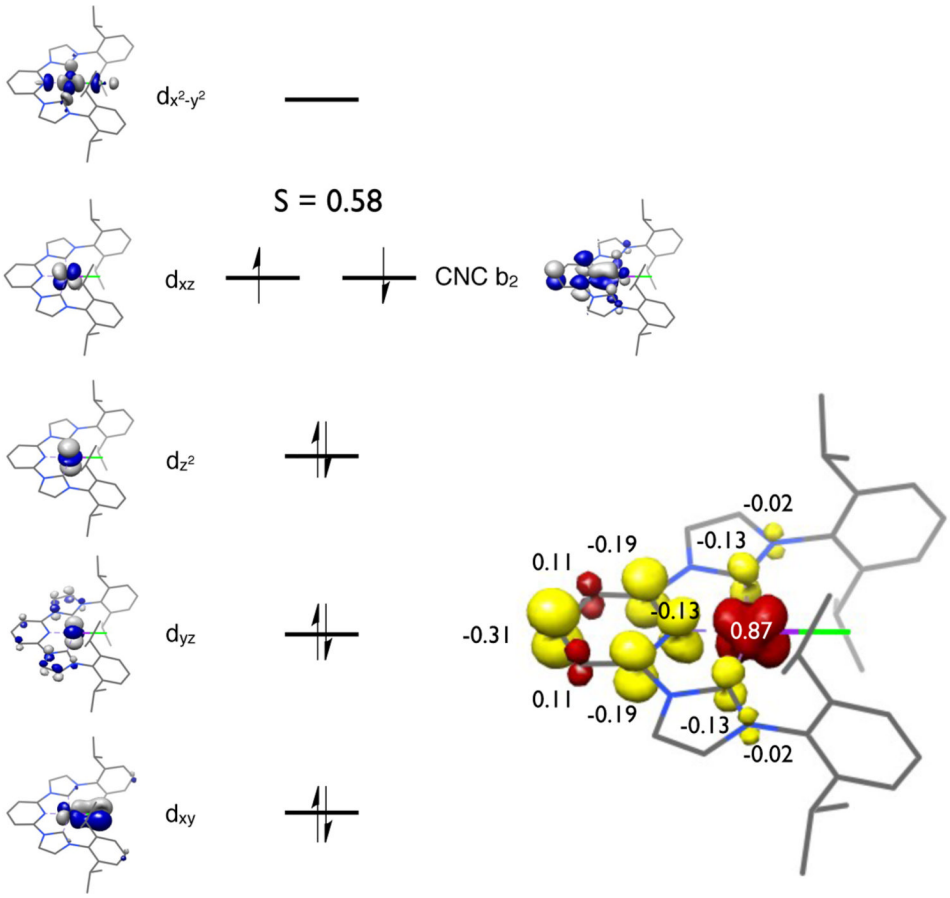

Figure 12.

Qualitative molecular orbital diagram (left) for (^{iPr}CNC)CoBr from a BS(1,1) calculation at B3LYP level. Spin density plot (right) was obtained from Mulliken population analysis (red, positive spin density; yellow, negative spin density).

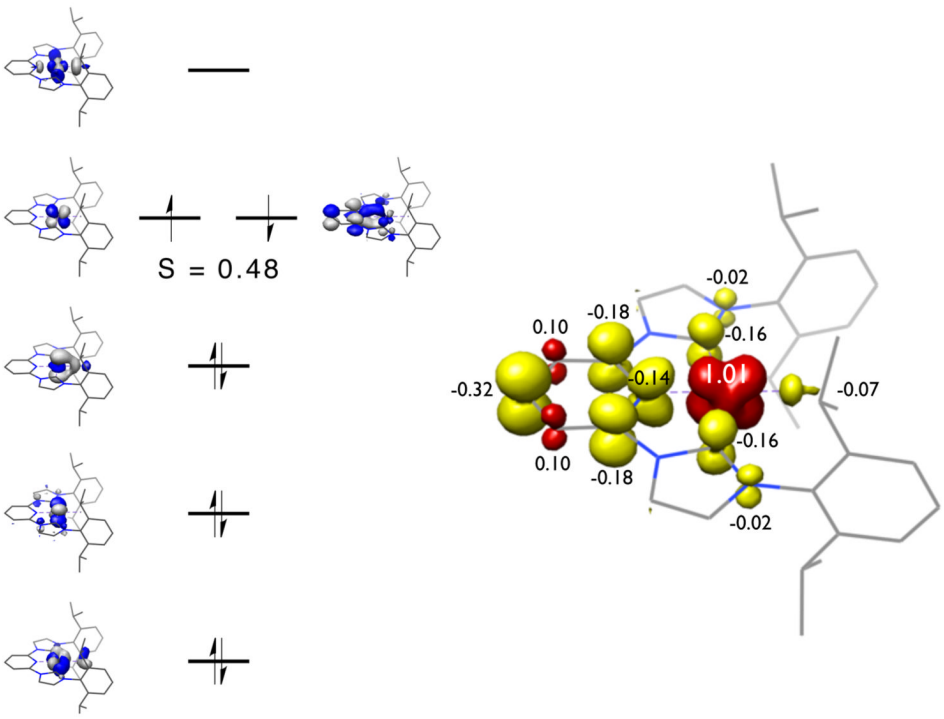

Figure 13.

Qualitative molecular orbital diagram for (^{iPr}CNC)CoCH$_3$ obtained from a BS(1,1) DFT calculation at the B3LYP level of DFT (left). Spin density plot for (^{iPr}CNC)CoCH$_3$ was obtained from a Mulliken population analysis (right).

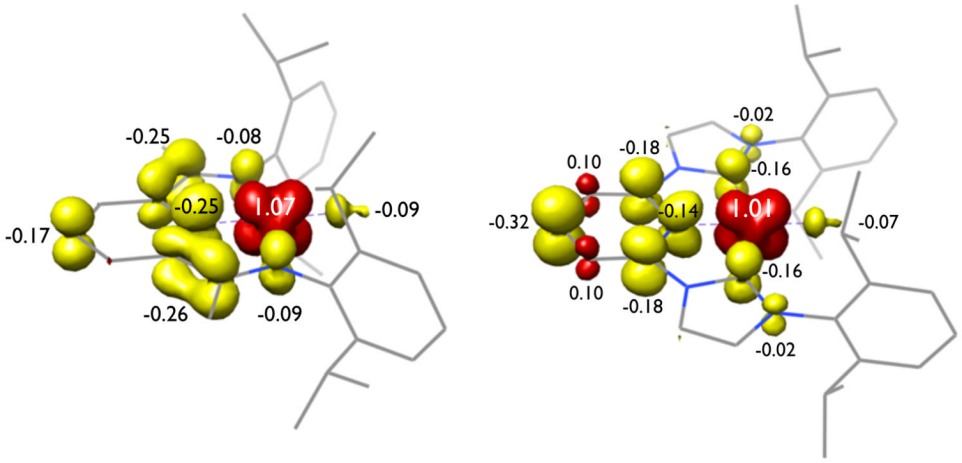

Figure 14.
Comparison of the spin density plots of (^{iPr}PDI)CoCH$_3$ (left) and (^{iPr}CNC)CoCH$_3$ (right).

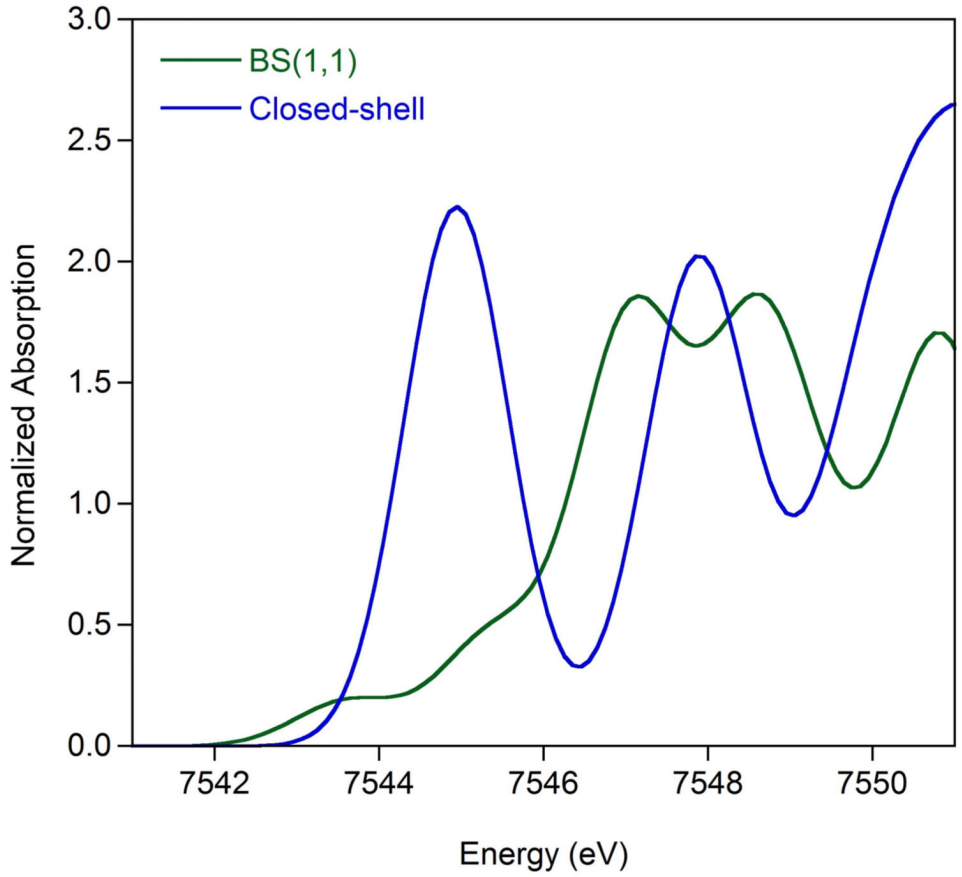

Figure 15.
Calculated XAS spectra of (^{iPr}CNC)CoBr and (^{iPr}CNC)$CoCH_3$ using the BP86 functional. A broadening of 1.5 eV has been applied to the computed spectra which have not been energy normalized.

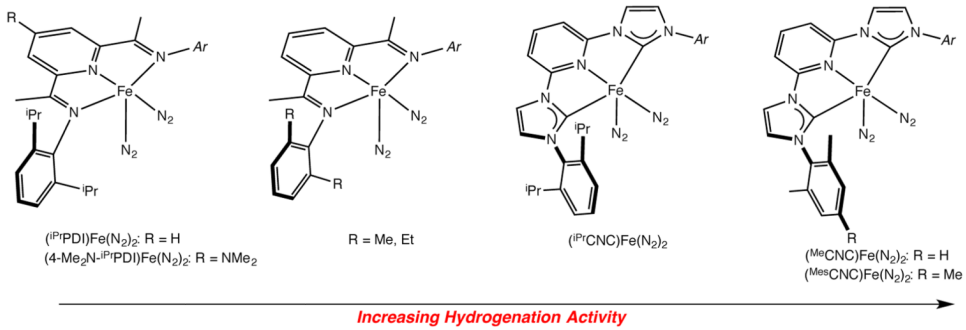

Scheme 1.

Bis(imino)pyridine and pyridine *N*-heterocyclic dicarbene iron dinitrogen complexes that are active pre-catalysts for olefin hydrogenation. The dimers, $[(^{R}PDI)Fe(N_2)](\mu_2\text{-}N_2)$ (R = Me, Et), are depicted as monomers for simplicity.

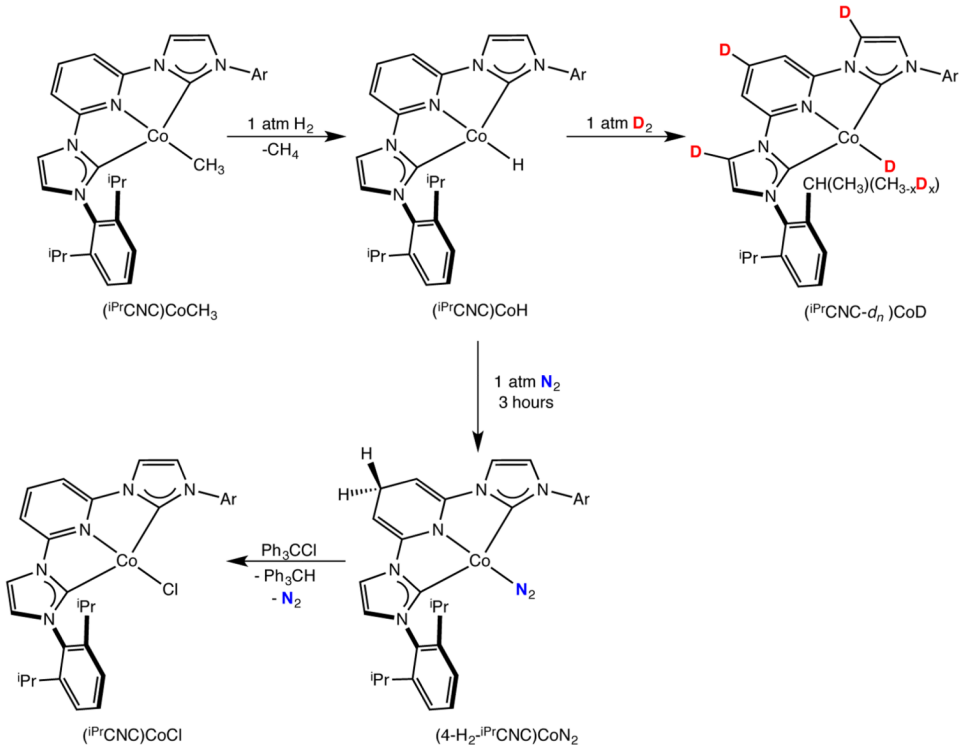

Scheme 2.
Synthesis and reactivity of a bis(arylimidazol-2-ylidene)pyridine cobalt hydride.

Table 1

Catalytic hydrogenation of alkenes with bis(arylimidazol-2-ylidene)pyridine cobalt and iron pre-catalysts

Entry[a]	Substrate	(^{iPr}CNC)CoCH$_3$	(^{iPr}CNC)Fe(N$_2$)$_2$
1[b]	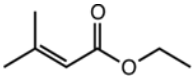	>95% (1 hr)	>95% (1 hr)
2[b]	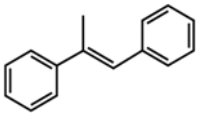	>95% (5 hr)	89% (12 hr)
3[c]	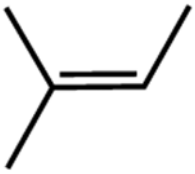	>95% (5 hr)	>95% (15 hr)
4[b]	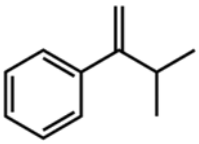	>95% (5 hr)	>95% (15 hr)
5[b,d]	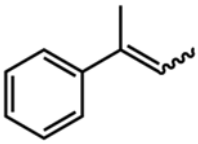	>95% (7 hr)	>95% (8 hr)
6[b]	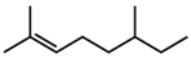	95% (13 hr)	>95% (18 hr)
7[b]	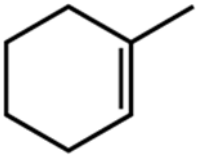	95% (120 hr)[e]	20% (24 hr)
8[c]	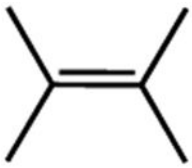	15% (24 hr)[f]	0% (24 hr)

[a] All catalytic reactions carried out with 5 mol% of the metal complex (0.032 mmol) in 0.916 M substrate benzene solution with 4 atm of H_2 at 22 °C.

[b] Conversions determined by GC-FID.

[c] Conversions determined by ^{1}H NMR spectroscopy.

[d] Substrate used as racemic mixture.

[e] 32% conversion at 12 hours.

[f] At 50 °C, conversion is 69% over 24 hours.

Table 2

Selected bond distances (Å) and angles (deg) for (4-CPh_2CH_3-^{iPr}CNC)CoN_2

Co(1)–N(3)	1.8553(16)
Co(1)–C(3)	1.9015(19)
Co(1)–C(9)	1.8980(19)
Co(1)–N(6)	1.7500(17)
C(4)–C(5)	1.333(3)
C(7)–C(8)	1.335(3)
C(5)–C(6)	1.513(3)
C(6)–C(7)	1.526(2)
N(1)–C(3)	1.357(3)
C(3)–N(2)	1.381(2)
N(4)–C(9)	1.377(2)
C(9)–N(5)	1.366(2)
N(6)–N(7)	1.112(2)
N(1)–C(3)–N(2)	103.67(15)
N(4)–C(9)–N(5)	103.28(16)

Table 3

Selected bond distances (Å) for (^{iPr}CNC), [(^{iPr}CNC)CoCH$_3$][BAr$^F_4$], [(^{iPr}CNC)CoN$_2$][BAr$^F_4$], (^{iPr}CNC)CoCl, (^{iPr}CNC)CoBr and (^{iPr}CNC)CoCH$_3$

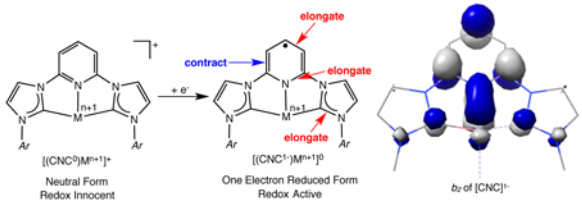

	(^{iPr}CNC)[a]	(^{iPr}CNC)CoMe$^+$	(^{iPr}CNC)CoN$_2^+$	(^{iPr}CNC)CoCl	(^{iPr}CNC)CoBr[b]	(^{iPr}CNC)CoMe[b]
Co–N$_{pyr}$		1.9193(13)	1.871(2)	1.832(2)	1.840(5)	1.865(3)
Co–C$_{carbene}$		1.9479(17)	1.913(3)	1.904(3)	1.918(6)	1.914(4)
		1.9432(17)	1.903(3)	1.907(3)	1.909(6)	1.898(4)
Co–X		1.9542(18)		2.2004(8)	2.3169(8)	1.951(4)
Co–N$_2$			1.801(3)			
N$_{pyr}$–C$_{ipso}$	1.327(4)	1.333(2)	1.340(4)	1.357(4)	1.353(7)	1.358(5)
	1.345(4)	1.335(2)	1.339(4)	1.369(4)	1.371(7)	1.357(5)
C$_{ipso}$–C$_{m\text{-pyr}}$	1.362(5)	1.382(3)	1.375(4)	1.367(4)	1.379(7)	1.373(7)
	1.388(5)	1.381(2)	1.383(4)	1.371(5)	1.378(8)	1.374(6)
C$_{m\text{-pyr}}$–C$_{p\text{-pyr}}$	1.387(5)	1.388(3)	1.384(5)	1.399(5)	1.397(9)	1.397(7)
	1.392(5)	1.389(3)	1.389(5)	1.392(5)	1.410(9)	1.416(6)
C$_{ipso}$–N$_{carbene}$	1.413(4)	1.399(2)	1.396(4)	1.393(4)	1.386(7)	1.394(5)
	1.427(4)	1.403(2)	1.404(4)	1.400(4)	1.387(7)	1.397(5)
N$_{carbene}$–C$_{carbene}$	1.372(4)	1.384(2)	1.373(3)	1.383(4)	1.388(6)	1.399(5)
	1.378(4)	1.382(2)	1.379(4)	1.380(4)	1.384(7)	1.400(5)
C$_{carbene}$–N$_{aryl}$	1.349(4)	1.346(2)	1.352(4)	1.364(4)	1.360(7)	1.375(6)
	1.359(4)	1.347(2)	1.348(4)	1.366(4)	1.364(7)	1.386(6)

[a] Data taken from reference 56.

[b] Data taken from reference 40.

Table 4

Cobalt K-edge parameters for bis(arylimidazol-2-ylidene)pyridine and bis(imino)pyridine cobalt halide and methyl compounds

Compound	Pre-edge Energy (eV)	Pre-edge Intensity A[a]	Pre-edge Intensity B[b]	Temperature (K)
(^{iPr}CNC)CoBr	7709.8	33(3)	42(3)	10
	7711.8	17(4)	7(1)	10
(^{iPr}CNC)CoCH$_3$	7709.7	29.8(6)	37.6(8)	10
	7711.2	5.8(8)	7(2)	10
(^{iPr}PDI)CoCl	7709.3	14.1(9)	18(1)	10
(^{iPr}PDI)CoCH$_3$	7709.3	13(1)	16(2)	10

[a] Fit using method described in reference 72.

[b] Fit using method described in reference 73.

Table 5

Comparison of various bis(arylimidazol-2-ylidene)pyridine cobalt precursors for the catalytic for the hydrogenation of *trans*-methylstilbene

Cobalt Compound	Solvent	Conversion[a,b]
(^{iPr}CNC)CoCH$_3$	C_6H_6	50%
(^{iPr}CNC)CoCH$_3$	C_6H_5F	14%
(4-H$_2$-^{iPr}CNC)CoN$_2$	C_6H_6	27%
[(^{iPr}CNC)CoN$_2$][BAr$^F_4$][c]	C_6H_6	27%
[(^{iPr}CNC)CoN$_2$][BAr$^F_4$]	C_6H_5F	6%

[a] All catalytic reactions carried out with 5 mol% of the metal complex (0.032 mmol) in 0.916 M substrate solution in the desired solvents with 4 atm of H_2 at 22 °C.

[b] Conversions determined by GC-FID.

[c] Generated in situ using (^{iPr}CNC)CoBr and 1.05 eq. NaBAr$^F_4$.